Repeated COVID-19 mRNA-based vaccination contributes to SARS-CoV-2 neutralizing antibody responses in the mucosa

Authors: Jozefien Declercq[1,2,3], Sarah Gerlo[4,5], Sharon Van Nevel[3], Natalie De Ruyck[3], Gabriele Holtappels[3], Liesbeth Delesie[5], Els Tobback[5], Inés Lammens[1,2,3], Nikita Gerebtsov[1,2], Koen Sedeyn[6,7], Xavier Saelens[6,7], Bart N. Lambrecht[1,2,8], Philippe Gevaert[3], Linos Vandekerckhove[5]†, Stijn Vanhee[1,2,3]†*

Affiliations:

[1] Laboratory of Mucosal Immunology, VIB Center for Inflammation Research, 9000 Ghent, Belgium.
[2] Department of Internal Medicine and Pediatrics, Faculty of Medicine and Health Sciences, Ghent University, 9000 Ghent, Belgium.
[3] Upper Airways Research Laboratory, Department of Head and Skin, Faculty of Medicine and Health Sciences, Ghent University, 9000 Ghent, Belgium.
[4] Department of Biomolecular Medicine, Ghent University, 9000 Ghent, Belgium.
[5] HIV Cure Research Center, Department of Internal Medicine and Pediatrics, Ghent University, 9000 Ghent, Belgium.
[6] VIB Center for Medical Biotechnology, 9000 Ghent, Belgium.
[7] Department of Biochemistry and Microbiology, Ghent University, 9000 Ghent, Belgium.
[8] Department of Pulmonary Medicine, Erasmus Medical Center, 3015 GD Rotterdam, the Netherlands.

†SV and LV are shared senior author

*Corresponding author. Email: Stijn.vanhee@ugent.be

One Sentence Summary: mRNA booster vaccines for SARS-CoV-2 induce circulating virus neutralizing antibodies that may enter the respiratory mucosa.

Abstract

To prevent infection by respiratory viruses and consequently limit virus circulation, vaccines need to promote mucosal immunity. The extent to which the currently used mRNA-based coronavirus disease 2019 (COVID-19) vaccines induce mucosal immunity remains poorly characterized. We evaluated mucosal neutralizing antibody responses in a cohort of 183 individuals. Participants were sampled at several timepoints after primary adenovirus vector- or mRNA-based COVID-19 vaccination, as well as after mRNA-based booster vaccinations. Our findings revealed that repeated vaccination with mRNA boosters promoted severe acute respiratory syndrome coronavirus 2 (SARS-CoV-2) neutralizing antibodies in nasal secretions. Nasal and serum neutralizing antibody titers correlated with one another, and were both of IgG and IgA isotypes. We investigated the source of these mucosal antibodies in a mouse model wherein mice received repeated mRNA vaccines for SARS-CoV-2. These experiments indicated that neutralizing antibody-producing cells reside in the spleen and bone marrow, whereas no proof of tissue homing to the respiratory mucosa was observed, despite the detection of mucosal antibodies. Serum transfer experiments confirmed that circulating antibodies were able to migrate to the respiratory mucosa. Collectively, these results demonstrate that, especially upon repeated vaccination, the currently used COVID-19 mRNA vaccines can elicit mucosal neutralizing, and that vaccination might also stimulate mucosal immunity induced by previously SARS-CoV-2 infection. Moreover, migration of circulating antibodies to the respiratory mucosa might be a main mechanism. These findings advance our understanding of mRNA vaccine-induced immunity and have implications for the design of vaccine strategies in combating respiratory infections.

INTRODUCTION

Vaccines are an effective tool in the battle against respiratory viruses, reducing morbidity and mortality associated with diseases caused by these pathogens (*1*). Ideally, vaccination should result in the elimination of the virus before it can infect host cells, a phenomenon referred to as sterilizing immunity. Neutralizing antibodies (Nabs) are generally seen as the major mediators of sterilizing immunity (*2-6*). However, T cells also contribute by eliminating infected host cells before the onset of new virus production (*3, 7*). As the airway mucosa serves as the first entry site for respiratory viruses, vaccination needs to induce robust immune responses in the respiratory mucosa to result in sterilizing immunity. Failure to achieve this allows for continued virus circulation with the risk for the emergence of new variants.

mRNA-based vaccines were introduced 30 years ago (*8*), but the severe acute respiratory syndrome coronavirus 2 (SARS-CoV-2) pandemic fueled their widespread use, leading to the current US Food and Drug Administration (FDA) approval of two coronavirus disease 2019 (COVID-19) mRNA vaccines. Both vaccines exhibit robust immunogenicity and are effective in preventing severe disease and mortality (*9-12*). However, whether mRNA vaccines induce long-lasting respiratory mucosal immunity remains a matter of debate. Several studies have reported on the induction of SARS-CoV-2-specific antibodies in nasal or oral samples to some extent after mRNA vaccination (*13-20*). Yet, this was not confirmed by others (*21-23*), potentially explained by different timing between sampling and vaccination, bias by prior SARS-CoV-2 infection, or different sampling and detection methods. Few have investigated the durability of this response, and most studied mucosal responses after two vaccinations, although standard regimens include further boosting of this response. In addition, the mechanisms by which mRNA vaccination might trigger mucosal immunity are currently unknown. As mRNA vaccination induces robust titers of systemic circulating antibodies, it is possible that these antibodies might enter the respiratory tissue through transudation or secretion (*24, 25*). Alternatively, some studies have suggested that mRNA vaccination can induce nasal virus NAb-secreting cells (*13, 25*). All these hypotheses remain to be formally investigated. A better understanding of the ability and mechanism by which mRNA-based vaccines promote mucosal immunity might enable further development of improved mRNA vaccines.

We took advantage of the global vaccination programs against SARS-CoV-2 to address the aforementioned questions. The present study involved a systematic sampling of individuals receiving multiple doses of mRNA-based vaccines. Specifically, we comprehensively characterized mucosal humoral responses in a cohort of 183 individuals that were prospectively sampled at multiple fixed time points after primary and booster vaccination. Using a mouse model, we further attempted to elucidate the mechanisms underlying mucosal neutralizing responses induced by mRNA vaccination. Our findings reveal that repeated mRNA vaccination was more potent at inducing robust and long-lasting mucosal neutralizing activity compared with primary vaccination. Moreover, prior natural SARS-CoV-2 infection appeared to enhance vaccine-induced respiratory virus neutralizing activity, especially in relation to the IgA response. Our mouse studies revealed that, in uninfected but vaccinated mice, most of mucosal NAbs were of systemic origin, and showed no detectable NAb-producing cells in the respiratory mucosa. Collectively, our data demonstrate that repeated mRNA vaccination induces systemic NAbs that can reach the respiratory mucosa.

RESULTS

Repeated mRNA vaccination induces SARS-CoV-2 NAbs in the nasal mucosa

We collected serum and nasal secretions before and at various time points after primary and booster vaccination (Fig. 1A). A total of 183 participants were sampled prior to and post primary vaccination and consequently included in the analysis (table S1). Of this group, 84 received 2 doses of the mRNA-based BNT162b2 vaccine and 99 two doses of the adenovirus vector (AVV)-based ChAdOx1 nCOV-19 vaccine. All study participants received their first vaccination dose in February or March 2021. At the timepoint of booster vaccination, 62 participants with primary mRNA-based vaccination and 80 participants with primary AVV-based vaccination were still in the study. All participants received an mRNA-based booster vaccination (BNT162b2: n=134; mRNA-1273: n=8) (Fig. 1A, table S1). Booster vaccinations were administered between September 2021 and January 2022.

We performed a surrogate virus neutralization test (*26*) on both serum and nasal secretion samples. Upon primary mRNA vaccination, all participants developed robust serum titers of SARS-CoV-2 NAbs, which declined 6 months after the second dose (Fig. 1B). In most mRNA vaccinated individuals, NAbs were also detected in nasal secretions. However, the titers declined 6 months later, going below the neutralization cut-off in more than half of the study participants. An mRNA-based booster vaccination increased nasal NAbs to a significantly (P <0.001) higher extent than primary vaccination. Additionally, average nasal antibody concentrations were higher 6 months after the booster than 6 months after primary vaccination (Fig. 1B), suggesting that repeated mRNA-based vaccination enhances mucosal neutralizing activity. Further, we observed that serum and nasal NAb titers significantly (r=0.77, p=<0.0001 after primary vaccination; r=0.74, p<0.001 after booster vaccination) correlated with one another at all time points (Fig. 1C, fig. S1A). A primary AVV-based vaccinated group was included in the study to investigate whether mRNA-based booster vaccination is as potent in a heterologous vaccination regimen as in a homologous vaccination regimen. Despite the differences in nasal NAb titers after primary mRNA- versus AVV-based vaccination (Fig. 1D), no differences in nasal NAb titers were observed between both groups after mRNA-based booster vaccination (Fig. 1E). A complete overview of NAb titer kinetics upon mRNA- versus AVV-based vaccination is provided in fig. S1B. Finally, as our study cohort included more females than males, we analyzed whether biological sex related differences exist in nasal NAb titers, but we did not observe differences (fig. S1C). Taken together, these data suggest that repeated mRNA vaccination augments the concentration of respiratory mucosal antibodies.

Prior COVID-19 enhances mucosal NAb titers upon vaccination.

It was previously reported that SARS-CoV-2 infection is required for robust virus neutralizing activity in the respiratory mucosa upon mRNA vaccination (*13, 19, 21, 22, 27*). To further explore the effects of previous natural infection, we measured nucleocapsid (N)-specific IgG titers in serum. Prior to any vaccination, 11% of primary mRNA vaccinated participants displayed anti-N IgG in the serum, indicative of prior SARS-CoV-2 infection (table S1). These participants exhibited significantly higher serum and nasal NAb titers at both 2 to 4 weeks (p=0.00020 for serum and p=0.0040 for nasal secretions) and 6 months (p=0.0050 for serum and p=0.0074 for nasal secretions) after primary mRNA-based vaccination (Fig. 2A). These trends were not

observed for nasal secretions of participants receiving primary AVV-based vaccination (fig. S2A). Participants with a rise in serum anti-N IgG titers after vaccination were excluded from this analysis. Nasal NAb titers induced by a third mRNA vaccination were not significantly ($P = 0.46$) affected by previous seroconversion of anti-N IgG (Fig. 2B). However, the potentiating effect of previous infection on heterologous booster induced NAb titers did display a statistically significant trend for presence of Nabs in both serum ($P = 0.0006$) and nasal secretions($P < 0.0001$) (Fig. 2C). We observed that 39% and 50% of homologous and heterologous mRNA boosted individuals, respectively, experienced natural SARS-CoV-2 infection after booster vaccination (based on a rise in serum anti-N IgG between 2 to 4 weeks and 6 months after booster vaccination) (table S1). As expected, upon categorizing participants with and without evidence of SARS-CoV-2 infection after booster vaccination, significantly higher titers of serum ($P = 0.038$ and $P < 0.0001$ for homologous and heterologous regimen respectively) and nasal ($P = 0.0010$ and $P = 0.00014$ for homologous and heterologous regimen respectively) NAbs were observed at 6 months post-booster vaccination in the first group (fig. S2B), confirming earlier observations that SARS-CoV-2 infection induces mucosal antibody responses (*21, 27*). To eliminate potential bias induced by higher rates of SARS-CoV-2 infection after booster compared to primary vaccination, we excluded those individuals that displayed a rise in anti-N IgG titers post booster vaccination (either at 2 to 4 weeks or 6 months after booster). Within this subgroup, a third mRNA vaccination still led to higher mucosal NAb titers at 6 months post vaccination compared with primary vaccination (fig. S2C), confirming that repeated mRNA vaccination induces larger mucosal humoral responses compared to primary vaccination, irrespective of prior infection.

Vaccine-induced virus NAbs are of IgG and IgA isotypes in both serum and nasal secretions

A previous study demonstrated that high titers of mucosal spike protein (S)-specific IgA induced by SARS-CoV-2 infection correlated with increased protection against reinfection by subsequent variants (*6, 28*). In contrast, this correlation was not observed concerning mucosal S-specific IgG titers, underlining the importance of mucosal IgA responses. Currently, there is uncertainty whether mRNA vaccines trigger mucosal IgA responses (*13, 16, 18, 19, 23, 29*). Our observation of enhanced neutralizing activity in the nasal mucosa following repeated vaccinations led us to hypothesize that multiple vaccinations might be required for a mucosal IgA response. To test our

hypothesis, we measured anti-S1 IgG and IgA titers in serum and nasal secretions of a subgroup of our study cohort (n=56, of which 34 mRNA vaccination as primary and 22 AVV vaccination). Anti-S1 IgA and IgG were detected in both serum and nasal secretions after mRNA vaccination (Fig. 3A and B). Whereas nasal anti-S1 IgG was detected in all study participants after both primary and booster vaccination, a subgroup did not have nasal anti-S1 IgA, even upon booster vaccination. No differences were observed between homologous and heterologous mRNA-based booster vaccination (Fig. 3C and D). An overview of anti-S1 IgG and IgA kinetics upon AVV-based vaccination is provided in fig. S3A and B. In line with the correlations observed for serum and nasal neutralizing activity, serum and nasal anti-S1 IgG and IgA titers correlated significantly with one another at all time points (for IgG: $P = 0.0030$ and $P < 0.0001$ for primary and booster vaccination respectively; for IgA: $P = 0.0004$ and $P < 0.0001$ for primary and booster vaccination respectively) (fig. S3C and D).

It is well-appreciated that the larger fraction of mucosal IgA is dimeric and transported from the basal to apical site of the mucosa by the polymeric immunoglobulin receptor (PIGR) (*30, 31*). During this process, the extracellular component of the PIGR, the secretory component, is incorporated into the IgA molecules. To explore whether mRNA vaccination induced mucosal antibodies that can be actively secreted by the PIGR, we measured S-specific secretory component-containing antibodies in nasal secretions as previously described by others (*13, 18*). We could indeed detect anti-S secretory component in some individuals, suggesting that at least a part of vaccination induced mucosal antibodies are actively secreted to the apical surface of the epithelium (fig. S3E). In addition, S-specific total IgA and secretory component-containing antibody concentrations correlated significantly to one another ($P = 0.0096$) (fig. S3F).

Given that we did not observe mucosal anti-S1 IgA in all participants, we questioned whether natural virus infection was required to prime vaccine-induced mucosal IgA. Whereas nasal anti-S1 IgG titers were not different between participants with and without evidence of natural infection (defined as seroconversion of anti-N IgG prior to vaccination), we did observe higher serum titers of anti-S1 IgA in those with prior SARS-CoV-2 infection (Fig. 3E to H). Nasal anti-S1 IgA was detected upon vaccination in almost all anti-N IgG positive participants, whereas this was not the case for all anti-N IgG negative participants (Fig. 3 G to H). Yet, half of the latter group also displayed nasal anti-S1 IgA, suggesting that mRNA vaccination can induce mucosal IgA responses. Of note, no clear differences in S-specific secretory antibodies were detected upon

primary vaccination between anti-N IgG seropositive and seronegative individuals (fig. S3G). Moreover, when correlating serum anti-N IgG titers with nasal anti-S1 IgA and IgG titers, we observe that anti-N IgG seropositive individuals or those with titers just below the cut-off have detectable nasal anti-S1 IgA, whereas nasal anti-S1 IgG titers were evident in all vaccinated individuals, irrespective of serum anti-N IgG titers (fig. S3H and I).

Further, 6 months after the booster, nasal anti-S1 IgG and IgA titers were higher than 6 months after the primary vaccination (Fig. 3A and C), and this difference remained significant ($P = 0.0010$ for IgG and P = 0.0014 for IgA) after excluding participants that exhibited a rise in anti-N IgG titers post booster vaccination (fig. S3J to M). These observations are in line with the NAb titer results (Fig. S2C). However, in contrast to the nasal NAb titers, nasal anti-S1 IgG and IgA titers were not significantly ($P > 0.99$ for both IgG and IgA) higher at early timepoints after booster vaccination compared to primary vaccination (Fig. 1B, Fig. 3A and C). This seeming discrepancy might be explained by enhanced affinity maturation upon prolonged antigen exposure, whereas secreted antibody titers remain stable (*32*-*35*). Taken together, these data show that mRNA vaccination promotes systemic and mucosal antibody responses of both IgG and IgA isotypes, and prior SARS-CoV-2 infection predominantly primes IgA responses both in serum and in the mucosa.

Repeated mRNA vaccination induces serum and BAL virus NAb in mice in the absence of detectable antibody producing cells in the respiratory mucosa

Next, we questioned how mucosal antibodies are induced by mRNA vaccination. Whereas Tang *et al.* did not detect S-specific IgA titers or B cells in the broncho-alveolar lavage (BAL) fluid of mRNA vaccinated mice (*17*), we did observe S-specific IgA in nasal secretions upon repeated vaccination in humans, even in the absence of anti-N IgG. As repeated mRNA-based vaccination was more potent at inducing mucosal humoral responses, we hypothesized that multiple immunizations might be required to promote homing of NAb producing plasma cells to the respiratory mucosa. As it is almost impossible to discriminate between infection- and vaccination-induced effects in humans, we used a mouse model of repeated mRNA-based immunizations to test our hypothesis (Fig. 4A).

One dose of mRNA-based vaccination was sufficient to induce neutralizing activity in the serum, whereas neutralizing activity in the BAL fluid was only detected after a second dose (Fig. 4B). In line with our observations in humans, serum and BAL S-specific antibodies were both of IgG and

IgA isotypes (Fig. 4C and D). For the induction of S-specific IgA antibodies, a minimum of 2 mRNA vaccinations were required, strengthening the idea that repeated immunizations are required to promote mucosal responses. A correlation between serum and nasal antibody titers was observed in this mouse model, similar to what we observed in human samples (fig. S4A).

Next, we investigated whether S-specific B cell responses are initiated upon repeated mRNA-based vaccination. Seven days after the last immunization, an enrichment of S-specific B cells was observed in the draining inguinal lymph node (iLN) and the spleen of vaccinated mice (Fig. 4E and F, fig. S4B). In both organs, a significant proportion of S-specific B cells displayed a germinal center phenotype ($CD95^+GI7^+$)($P = 0.016$ for iLN, $P = 0.032$ for spleen), whereas those were not observed in naïve mice. In addition, S-specific plasmablasts/plasma cells (PBPCs) were detected in the iLN and spleen of vaccinated mice. No enrichment of S-specific B cells, S-specific germinal center B cells or S-specific PBPCs could be found in non-draining mediastinal lymph nodes (mLN), nor in the respiratory mucosa, even not after 4 immunizations (Fig. 4F). Taken together, repeated mRNA vaccination induces S-specific B cell activation in the draining lymph node, and possibly in the spleen, where S-specific B cells might also be recirculating cells from the draining lymph node.

Finally, we investigated by flow cytometry where S-specific PBPCs reside after exiting the germinal center reaction. S-specific PBPCs were detected predominantly in the spleen and bone marrow at 21 days after the last vaccination, whereas none were found in the respiratory mucosa (Fig. 4G and H, fig. S4C). To confirm the absence of mucosal plasma cells by a more sensitive method, and to determine the isotypes of the antibody secreting cells (ASC), we performed ELISPOT on bone marrow and lung samples. The blood-derived fraction was removed from the lung cells by magnetic depletion of intravenously (IV) labeled cells (fig. S4D). Detection of ASCs in blood-depleted lung single cell suspensions by a kappa/lambda-coated ELISPOT assay excluded that ASCs were dying as a result of the sorting process (fig. S4E). S-specific IgG and IgA ASCs were found in the bone marrow, but not in the lung mucosa, including after 2 and after 4 vaccinations (Fig. 4I and J, fig. S4F and G).

Since we did not detect any mucosal S-specific ASCs, it is suggested that mucosal virus neutralizing activity originated from the serum compartment. To confirm that systemically produced antibodies traffic from the serum compartment to the respiratory mucosa, we transferred serum from twice vaccinated (shown to induce high titers of serum NAbs, Fig. 4B) and control

mice into naive recipients, and analyzed these 20 hours after transfer (Fig. 4K). Mice receiving serum from immunized mice displayed SARS-CoV-2 neutralizing activity in the serum, as well as in the BAL fluid, whereas recipients of control serum did not (Fig. 4L). Analysis of S-specific IgG and IgA titers showed that mainly IgG contributes to mucosal virus neutralizing activity (fig. S4H and I). S-specific IgA was not detected in BAL fluid, nor in serum of recipients of immunized serum. However, at an earlier timepoint after serum transfer (5 hours), traces of S-specific IgA were detected in the serum of recipients of immunized serum (fig. S4J), suggesting that the efficacy of IgA transport to the respiratory mucosa is rather inefficient at low serum concentrations. Taken together, these data demonstrate that mRNA-based vaccines induce systemic NAbs that might provide mucosal immunity. Repeated immunizations enhance serum NAb titers, with consequently increased mucosal neutralizing responses.

DISCUSSION

Ideally, vaccines protect not only against severe disease, but also against infection to limit virus circulation. Achieving this goal requires the induction of mucosal immunity through vaccination. In the present study, we comprehensively characterized humoral responses in the airway mucosa upon mRNA-based vaccination. Our findings demonstrate that repeated vaccination in particular induces mucosal virus neutralizing activity. This mucosal neutralizing activity wanes as serum titers decrease. Both virus-specific IgA and IgG are produced systemically and can be detected in the airway mucosa. However, whereas mucosal virus-specific IgG antibodies were measured in the majority of repeatedly-vaccinated individuals, the mucosal IgA response upon vaccination was found to be more variable. Our mouse studies suggest that mucosal neutralizing activity mainly originates from circulating antibodies that traffic to the respiratory mucosa. Even upon repeated immunizations, no mucosal origin of respiratory antibodies was identified.

Many studies have documented the capacity of mRNA-based vaccines to provoke mucosal humoral responses (*13-19*), yet a few discrepant findings were reported. First, some studies did not detect any mucosal virus neutralizing activity (*21, 22*), possibly due to timing, sample or analytical techniques, and limited booster immunizations. Second, whether mRNA-based vaccination can prompt the production of mucosal IgA independent of infection remains a matter of debate. Evidence suggests that mucosal IgA plays a more crucial role in protecting against re-infection compared to mucosal IgG (*6, 28, 36*). Several studies could not detect clear titers of

vaccine-induced mucosal IgA in SARS-CoV-2 naïve individuals, whereas they did in SARS-CoV-2 convalescent individuals (*13, 17, 19, 22, 23*). Based on these findings, it was hypothesized that mRNA vaccination boosts mucosal recall responses primed by infection. However, others reported on vaccination-induced mucosal IgA responses in SARS-CoV-2 naïve individuals (*16, 18, 20*). We also observed mucosal virus-specific IgA in approximately half of anti-N IgG negative study participants. Yet, it cannot be ruled out that some of the anti-N IgG negative individuals did experience SARS-CoV-2 infection, given that seroconversion to anti-N does not always occur after SARS-CoV-2 infection, especially not in vaccinated individuals (*37*). Moreover, we cannot exclude the possibility that this observation is due to reactivation of mucosal recall responses primed by infection with other coronaviruses. Our mouse model demonstrates that mucosal virus-specific IgA can be induced by mRNA-based vaccination independent of prior infection, if serum IgA titers are high enough. Yet, it needs to be mentioned that substantial differences exist between mouse and human IgA; whereas IgA in serum of mice is mostly dimeric, it is mostly monomeric in human serum. In addition, whether intramuscular mRNA vaccination can reactivate mucosal memory responses remains to be investigated.

Our study provides mechanistic insights into how mRNA-based vaccines may provoke mucosal immunity. By inducing high serum titers of NAbs that traffic to the respiratory mucosa, mRNA-based vaccination might induce mucosal neutralizing responses, although they did not appear to be long-lasting. The correlations between serum and nasal virus-specific antibodies suggest a serum threshold might exist beyond which circulating antibodies migrate to the respiratory mucosa. This might also explain why AVV-based vaccines are less potent at inducing mucosal neutralizing activity, since these are known to induce lower serum NAb concentrations compared with mRNA-based vaccines (*38*). The mechanisms by which circulating antibodies are transported to the respiratory mucosa remain to be elucidated. The detection of S-specific secretory component in nasal secretions suggests that a fraction of the vaccination-induced IgA is transported from the basal to the apical site of the mucosa by the PIGR. Since most serum IgA is monomeric, passive transudate of SARS-CoV-2 S-specific IgA might also contribute. However, to which extent passive transudate of circulating IgA contributes to the mucosal IgA pool upon vaccination remains to be elucidated. Concerning mucosal IgG, active transport of IgG antibodies has been described through the neonatal Fc receptor (FcRn) (*30, 31*), although whether vaccination-induced

IgG migrates to the airways through passive transudation or rather active secretion remains to be studied.

Importantly, we use two different techniques to detect S-specific B cells, yet it cannot formally be ruled out that mRNA-based vaccination induces any undetected discrete seeding of S-specific PBPCs to the respiratory mucosa. In addition, our mechanistic findings are based on a mouse model, which might not completely recapitulate the human situation. Moreover, many humans might have been exposed to cross-reactive coronaviruses with consequent mucosal homing of SARS-CoV-2 cross-reactive PBPCs that might be reactivated by mRNA-based vaccination. The latter hypothesis was not tested in our study, but it would be important for fully understanding the mechanisms that lead to mucosal protection of mRNA vaccines.

Whereas all study participants displayed virus neutralizing responses in the nasal cavity upon a third mRNA vaccination, approximately half of them experienced a breakthrough infection during the following 6 months. This is at least partly due to the circulation of antibody escaping variants. Indeed, the time of booster vaccination in our cohort coincided with the emergence of omicron variant of SARS-CoV-2, which readily evades antibody-mediated neutralization (*13, 16, 18*). However, antibody-escaping variants cannot completely explain the high rate of breakthrough infections with the current mRNA vaccines. Waning vaccine effectiveness against infection is observed independent of variants (*39, 40*). Although mRNA vaccines initially induce high serum NAb titers, these decrease over time and correlate with waning protection against infection (*41-45*). Our data provide a mechanistic explanation for the observed waning vaccine effectiveness against infection: as high serum NAb titers are required for mucosal immunity upon mRNA-based vaccination, decreasing serum antibody titers are associated with a compromised mucosal immunity barrier, facilitating breakthrough infections.

Taken together, the current mRNA-based vaccination strategies might benefit from adaptations that promote more long-lasting mucosal immunity. The induction of robust cellular immunity in the mucosa might be advantageous. To achieve this goal, a thorough understanding of mucosal immunity is required. It is generally accepted that tissue homing of T and B cells is determined by the expression of homing receptors and adhesion molecules, which enable migration and retaining of the cells in the peripheral tissues (*46, 47*). Given that the imprinting of these homing receptors is determined by the anatomical site of induction, mucosal vaccination is an attractive strategy. Currently, 9 mucosal vaccines are approved, of which 8 oral vaccines and 1 intranasal live

attenuated influenza vaccine (LAIV) (*48*). Although an active area of research, the lack of approved mucosal adjuvants and the greater susceptibility to degradation and clearance of mucosal vaccines precludes their widespread use. The SARS-CoV-2 pandemic fueled the development of viral vector vaccines, which have been regarded as good platforms for mucosal vaccination as they mimic natural infection. Pre-clinical animal studies yielded promising results with intranasal SARS-CoV-2 vaccines (*49*). However, despite a favorable safety profile, most clinical trials observed only weak mucosal and systemic immunogenicity (*50-52*). The immunogenicity of mucosal vaccines might be enhanced with the development of mucosal adjuvants. Of note, mRNA formulations might also be used as mucosal vaccination platforms by adapting their carriers (*48, 53*). In addition, some studies have reported on the potential of parenteral immunization to induce mucosal cell-mediated immunity (*54, 55*). As we and others (*13, 20*) observed an increased potential for mRNA vaccines to induce mucosal IgA in previously SARS-CoV-2 infected individuals compared to controls, these vaccines might boost previously imprinted cellular mucosal immunity. Consequently, rational booster vaccinations of previously-infected individuals might also be a strategy to induce robust cellular mucosal immunity. However, this needs further investigation in future studies. In anticipation of vaccination strategies that induce robust mucosal cellular immunity, our study shows that a rational booster scheme is important for maintaining mucosal virus neutralizing antibodies.

Although this study expands our knowledge on mucosal antibody responses induced by mRNA vaccination, it also has some limitations. First, we used a surrogate virus neutralization test, which measures the presence of antibodies that block the interaction between the receptor binding domain (RBD) of the S protein and the host angiotensin converting enzyme 2 (ACE2) receptor, rather than a live virus neutralization assay. In comparison to classical ELISA-based methods, this technique allows to specifically measure neutralizing antibodies instead of the total pool of binding antibodies. In comparison with the gold standard conventional virus neutralization assays, neutralizing antibodies that are not RBD-binding are not detected by this assay. However, this surrogate virus neutralization assay has been extensively validated and was shown to correlate well with the results obtained by classical virus neutralization assays (*26*). Further, we did not assess the neutralization of different SARS-CoV-2 variants. Consequently, we cannot conclude whether breakthrough infections are due to a qualitative or quantitative deficit in mucosal NAbs. Second, our study population is a quite homogeneous population of predominantly healthy, relatively

young individuals with limited ethnic diversity. Future studies should investigate whether mucosal immunity might be hampered by age, comorbidities, or ethnicity.

Based on our data, repeated vaccination with the current mRNA-based vaccines enhances mucosal NAb titers; however, these responses are not long-lasting. We provide mechanistic evidence on how the currently used mRNA-based vaccines might induce mucosal immunity. Although we cannot formally rule out the possibility of mucosal homing of S-specific PBPCs induced by mRNA-based vaccination, our mouse data suggest that the majority of mucosal NAb are coming from the circulatory compartment. When serum antibody titers decline, mucosal immunity wanes as well, possibly explaining the waning vaccine effectiveness against infection. Future research should focus on modifications of vaccination strategies that promote robust induction of longer-lasting cellular mucosal immunity.

MATERIALS AND METHODS

Study design

This study aimed to gain more insight into the immune responses at the mucosal (nasal) and systemic (blood) level of healthy participants vaccinated with the current available COVID-19 messenger ribonucleic acid (mRNA; BNT162b2) and viral-vector based (ChAdOx1) vaccines. Individuals vaccinated at the COVID-19 vaccination center at the University Hospital Ghent, Belgium were recruited for our study. We obtained serum and nasal secretions from study participants prior to COVID-19 vaccination, 2 to 4 weeks and 6 months after two vaccine doses, and 2 to 4 weeks and 6 months after booster vaccination. Primary vaccination included either 2 doses of the Pfizer-BioNTech BNT162b2 mRNA-based vaccine or 2 doses of the AstraZeneca ChAdOx1/nCov-19 an AVV-based vaccine. Booster vaccination was performed with an mRNA-based vaccine (Pfizer-BioNTech BNT162b2 (n=134) or Moderna mRNA-1273 (n=8)). The study was approved by the competent authorities and the Ethical Committee of Ghent University Hospital, and was done in accordance with Good Clinical Practice guidelines and the Declaration of Helsinki. Every participant provided written informed consent for participation. Full cohort and demographic information is provided in table S1. All animal procedures performed in this study were approved by the animal ethical committee of Ghent University. Minimal group sizes to obtain

a power > 0.8 and an alpha error probability of 0.05 for the murine studies were calculated in G*Power (v3.1). Group sizes were based on the readout with the smallest effect size. Mouse experiments were repeated as indicated in the figure legends. No blinding was applied to the mouse experiments. No outliers were removed from the dataset.

Collection of nasal secretions

Collection of nasal secretions was performed as previously described (*56, 57*). Briefly, sinus packs were placed in the nasal cavity for 5 minutes and subsequently transferred to a 15 mL tube. Two mL physiologic saline (0.9% NaCl) was added, whereafter the sinus packs were incubated at 4°C for 2 hours. Next, sinus packs were transferred in 5 mL syringes, which were consequently put in a 15 mL tube and centrifuged.

Surrogate virus neutralization assay

SARS-CoV-2 NAbs were measured by a surrogate virus neutralization test (Elabscience; E-EL-E608) as per manufacturer's instructions. Briefly, human and mouse serum samples were diluted 5 and 50 times, respectively, and further diluted until falling in the range of the standard curve. Nasal secretions and BAL fluid were analyzed undiluted. Samples were incubated together with horseradish peroxidase (HRP) conjugated recombinant SARS-CoV-2 RBD on plates pre-coated with recombinant human ACE2. NAbs in the samples compete with the plate-bound ACE2 for sites on the HRP-RBD fragment. After incubation, the excess HRP-RBD, as well as any HRP-RBD-NAb complexes, are removed during washing. After developing the enzyme- 3,3′, 5,5′ tetramethylbenzidine (TMB) substrate reactions, plates were analyzed at 450 nm on a Multiskan FC Microplate Photometer (Thermo Fisher Scientific). For human samples, neutralization threshold was based on 10 pre-COVID-19 serum and nasal secretion samples (threshold was calculated as mean + 3x standard deviation). NAb titers were extrapolated from the standard curve obtained from the reference standard.

Recombinant S protein production

Recombinant SARS-CoV-2 S protein was produced and purified as previously described (*58*). The ectodomain of the SARS-CoV-2 S protein (ancestral Wuhan strain-derived, 2P, and mutated polybasic furin cleavage site) was expressed as a soluble, secreted protein, with a foldon-trimerization domain followed by a PreScission Protease cleave site, a His tag and two StrepII tags (WSHPQFEK) fused to the C-terminus. The protein was expressed by transiently transfected ExpiCHO cells and purified using a HisTrapHP column. For flow cytometry, S-trimers were assembled into tetramers, yielding 12-mer recombinant proteins. These were biotinylated, and consequently incubated with SAV-conjugated phycoerythrin (PE) by the VIB protein core facility.

Anti-SARS-CoV-2 nucleocapsid IgG ELISA

The presence of anti-SARS-CoV-2 nucleocapsid immunoglobulins in serum was determined with the anti-SARS-CoV-2 N protein human IgG ELISA kit (Proteintech; #KE30001). The assay was performed per manufacturer's instructions. Serum samples were diluted 100 times.

Human Anti-S1 IgG and IgA ELISA

Anti-S1 IgG and IgA ELISA kits (EUROIMMUN; EI 2606-9601 G/A) were performed on serum and nasal secretions as per manufacturer's instructions. A standard curve was obtained by a pool of serum samples with high SARS-CoV-2 NAb titers, from which arbitrary units (AU) were determined. Nasal secretions and serum samples were diluted 2 times, and further diluted until falling in the range of the standard curve. Plates were analyzed at 450 nm on a Multiskan FC Microplate Photometer. Background reference, measured at 620 nm, was subtracted.

Anti-S secretory component ELISA

S protein-specific secretory component antibodies were measured in nasal secretions as previously described by Sano et al. (*13*). Briefly, ELISA plates were coated with 500x diluted recombinant SARS-CoV-2 S protein (Bio-techne; 10549-CV-100). Blocking was performed with 5% non-fat milk in phosphate-buffered saline (Gibco) with Tween 20 (PBST; Merck-Sigma) for 1 hour. Nasal secretions were 2x diluted in 2.5% non-fat milk in PBST and incubated overnight at 4°C. Detection was performed with a mouse anti-human secretory IgA antibody at 5 µg/mL (Merck-Sigma;

411423-400UG), followed by the incubation with a 1000x diluted HRP-labeled goat anti-mouse IgG Fc antibody (Life Technologies; 14200-067). TMB substrate solution (Biotechne; DY999) was added, and plates were analyzed at 450 nm on a Multiskan FC Microplate Photometer. Background reference, measured at 620 nm, was subtracted.

Mouse studies

Female C57BL/6J wild-type mice were purchased from Janvier. Mice were bred and housed under specific pathogen-free conditions. Six- to 10-week old mice were vaccinated intramuscularly in the right hind leg with one, two, three, or four doses of 2 µg (in 50 µL Tris buffered saline) of the BNT162b2 vaccine. Repeated vaccinations were performed with a 21-day interval. Control mice received 50 µL Tris buffered saline intramuscularly. For serum transfers, 200 µL serum (of twice vaccinated mice) was intravenously injected in the tail veins of naive recipient mice. Mice were randomly assigned to their respective groups. Before euthanasia, mice were intravenously injected with 2 µg biotin-labeled anti-CD45 antibody (eBioscience; 13-0451-85) diluted in 100 µL phosphate-buffered saline (PBS) to discriminate between blood- and tissue-derived cells. For collection of BAL fluid, lungs were lavaged with 1 mL of EDTA-containing PBS (0.5 mmol/L), injected 3 times. Cells were recovered by centrifugation and stained for flow cytometry. Supernatant was stored at -20°C for further analysis. Blood was obtained from the iliac vein in noncoated Eppendorf tubes to prepare serum. Single-cell suspensions from iLN and mLN, and spleens were obtained by homogenizing the organ through a 100 µm cell strainer (Falcon). Bone marrow was collected by flushing the tibia and femur with PBS over a 100 µm cell strainer. Spleen and bone marrow red blood cells were lysed after centrifugation by an incubation step in 2 mL ammonium-chloride-potassium lysis buffer (10 mM KHCO3, 155 mM NH4Cl, 0.1 mM EDTA in Milli-Q water) for 2 minutes. The red blood cell lysis was stopped by adding a large volume of PBS. The left lung lobe was cut into small pieces. After adding RPMI-1640 (Gibco), these were smashed over a 100 µm cell strainer to obtain a single-cell suspension. Single-cell suspensions were centrifuged and red blood cell lysis was performed as described above. After adding a large volume of PBS and centrifugation, cells were stained for flow cytometry. For ELISPOT, lungs were cut in small pieces and incubated at 37°C for 30 minutes in RPMI-1640 containing 20 µg/mL Liberase TM (Roche), 10 U/mL DNase I (Roche), and 5% newborn calf serum. The digestion

reaction was stopped by the addition of a large volume of PBS. Lungs were filtered over a 100 µm cell strainer and cells were centrifuged. After osmotic lysis, cells were magnetically depleted of the IV-labeled fractions according to the MojoSort protocol. Briefly, cells were resuspended in 100 µL sort buffer [0.5% bovine serum albumin (BSA) and 2 mM EDTA in PBS], and incubated with 10 µL streptavidin (SAV)-conjugated magnetic beads (BioLegend) for 15 minutes on ice. Next, the volume was added to 2.5 mL with sort buffer, and tubes were placed in a MojoSort magnet (BioLegend) for 5 minutes at room temperature. After retrieval of negatively selected cells, again 2.5 mL sort buffer was added to the tube, and the magnetic sorting was repeated. The negative selected cells (blood depleted fraction) were used for ELISPOT analysis.

Mouse Anti-S IgG and IgA ELISA

ELISA plates were coated with anti-mouse IgG (Jackson ImmunoResearch; 315-005-008) and anti-mouse IgA (BD Biosciences; 556969) capture antibodies. Serum samples were diluted 200x, BAL samples were incubated undiluted. Detection was performed using recombinant S protein with StrepII tags. After incubation with HRP-conjugated SAV (BD Biosciences; 554066), TMB substrate was added. Plates were analyzed at 450 nm on a Tecan infinite 200 Pro reader. Reference absorbance, measured at 650 nm, was subtracted.

Flow cytometry

Lung, bone marrow, spleen, iLN and mLN single cells were first stained in 50 µL PBS containing the fixable viability dye eFluor506 (1:400; eBioScience; 65-0866-18), an FcγRII/III antibody (1:400; clone 2.4G2, provided by L. Boon, Bioceros) and allophycocyanin (APC)-conjugated SAV (1:1000; eBioscience; 17-4317-82) for 30 minutes at 4°C. After washing, surface staining was continued for 30 minutes at 4°C in 50 µL PBS containing the following antibodies: lineage antibodies [anti-CD4 fluorescein isothiocyanate (FITC; 1:200; clone RM4-5; eBioscience; 11-0042-85), anti-CD8a FITC (1:200; clone 53-6.7; BD Biosciences; 553031), anti-Ter119 FITC (1:200; clone TER-119; eBioscience; 11-5921-82), and anti-F4/80 Alexa Fluor (AF) 488 (1:200; clone BM8; eBioscience; 53-4801-82)], anti-CD80 peridinin-chlorophyll-protein (PerCP)-Cyanine (Cy)5.5 (1:100; clone 16-10A1; BioLegend; 104722); anti-Gl7 pacific blue (1:200; clone

Gl7; BioLegend; 144614); anti-CD45R/B220 brilliant violet (BV) 650 (1:200; clone RA3-6B2; BioLegend; 103241); anti-CD138 BV711 (1:100; clone 281-2; BioLegend; 142519); anti-CD19 BV786 (1:200; clone 1D3; BD Biosciences; 563333); anti-Sca1 AF700 (1:50; clone D7; BioLegend; 108142); anti-CD95 PE-Cy7 (1:200; clone Jo2; BD Biosciences; 557653); and anti-CD273 brilliant ultraviolet (BUV) 395 (1:200; clone TY25; BD Biosciences; 565102). PE-conjugated S protein 12-mer were added to the second staining mix to identify SARS-CoV-2 S-specific B cells. To eliminate B cells reactive for PE or other components of the complex, a Biotin-SAV-PE-AF647 decoy was used. After washing in PBS, cells were resuspended in 100 µL PBS and acquired on a Fortessa 5-laser instrument (BD Biosciences). Data were processed using FlowJo. Absolute numbers were calculated using precision count beads (BioLegend; 424902). A representative gating strategy is provided in fig. S5.

ELISPOT

ELISPOT plates (Millipore) were coated overnight with recombinant S protein (R&D Systems; 10549-CV) or with anti-light chain κλ (ELISPOT kit CTL; mIgAIgG-DCE-1M/5) for positive controls. The next day, plates were washed and incubated with assay medium (RPMI-1640 with 2 mM L-glutamine, 50 µM beta-mercaptoethanol, 8 µM HEPES, 100 U/mL penicillin, 100 µg/mL streptomycin, 10% fetal bovine serum) for 1 hour at room temperature. Lung and bone marrow cells were counted using a Bürker-Türk counting chamber. A maximum of $2.5x10^5$ cells per well were plated. Plates were incubated overnight at 37°C with 5% CO2. The next day, plates were washed and incubated with detection antibody for 2 hours [for IgA ELISPOT: FITC-conjugated anti-IgA supplied in the mouse IgG/IgA double color ELISPOT kit (CTL; mIgAIgG-DCE-1M/5)); for IgG ELISPOT: HRP-conjugated anti-mouse IgG (Jackson ImmunoResearch; 115-035-146]. For IgA ELISPOT, plates were incubated for 1 hour with HRP-conjugated anti-FITC antibody for 1 hour [supplied in mouse IgG/IgA double color ELISPOT kit (CTL; mIgAIgG-DCE-1M/5)]. Next, plates were developed with reagents from mouse IgG/IgA double color ELISPOT kit per manufacturer's instructions. Plates were analyzed on a CTL S6 Ultimate Analyzer using the ImmunoSpot 7 software (CTL).

Statistical analysis

Individual-level data are presented in data files S1 to S3. Statistical tests are indicated in the figure legends. Kruskal-Wallis test was used for multigroup comparisons with Dunn's correction for multiple testing. Mann-Whitney U test was used for comparing two groups, using Holm-Sidak correction for multiple testing where indicated. Correlations were tested by a two-sided Spearman correlation test. The statistical significance threshold was determined on $p < 0.05$. Significance values are indicated by $*p < 0.05$, $**p < 0.01$, $***p < 0.001$, and $****p < 0.0001$; ns, not significant. All statistical tests were performed in GraphPad Prism software.

List of Supplementary Materials

Supplementary Methods

Fig. S1 to S5

Table S1

Data files S1 to S3

References and Notes

1. O. J. Watson, G. Barnsley, J. Toor, A. B. Hogan, P. Winskill, A. C. Ghani, Global impact of the first year of COVID-19 vaccination: a mathematical modelling study. *Lancet Infect Dis* **22**, 1293-1302 (2022).
2. I. Wahl, H. Wardemann, Sterilizing immunity: Understanding COVID-19. *Immunity* **55**, 2231-2235 (2022).
3. K. McMahan, J. Yu, N. B. Mercado, C. Loos, L. H. Tostanoski, A. Chandrashekar, J. Liu, L. Peter, C. Atyeo, A. Zhu, E. A. Bondzie, G. Dagotto, M. S. Gebre, C. Jacob-Dolan, Z. Li, F. Nampanya, S. Patel, L. Pessaint, A. Van Ry, K. Blade, J. Yalley-Ogunro, M. Cabus, R. Brown, A. Cook, E. Teow, H. Andersen, M. G. Lewis, D. A. Lauffenburger, G. Alter, D. H. Barouch, Correlates of protection against SARS-CoV-2 in rhesus macaques. *Nature* **590**, 630-634 (2021).
4. Z. Ku, X. Xie, E. Davidson, X. Ye, H. Su, V. D. Menachery, Y. Li, Z. Yuan, X. Zhang, A. E. Muruato, I. E. AG, B. Tyrell, K. Doolan, B. J. Doranz, D. Wrapp, P. F. Bates, J. S. McLellan, S. R. Weiss, N. Zhang, P. Y. Shi, Z. An, Molecular determinants and mechanism for antibody cocktail preventing SARS-CoV-2 escape. *Nat Commun* **12**, 469 (2021).
5. Z. Ku, X. Xie, P. R. Hinton, X. Liu, X. Ye, A. E. Muruato, D. C. Ng, S. Biswas, J. Zou, Y. Liu, D. Pandya, V. D. Menachery, S. Rahman, Y. A. Cao, H. Deng, W. Xiong, K. B. Carlin, J. Liu, H. Su, E. J. Haanes, B. A. Keyt, N. Zhang, S. F. Carroll, P. Y. Shi, Z. An, Nasal delivery of an IgM offers broad protection from SARS-CoV-2 variants. *Nature* **595**, 718-723 (2021).
6. S. Havervall, U. Marking, J. Svensson, N. Greilert-Norin, P. Bacchus, P. Nilsson, S. Hober, M. Gordon, K. Blom, J. Klingstrom, M. Aberg, A. Smed-Sorensen, C. Thalin, Anti-Spike Mucosal IgA Protection against SARS-CoV-2 Omicron Infection. *N Engl J Med* **387**, 1333-1336 (2022).
7. P. S. Arunachalam, T. P. Charles, V. Joag, V. S. Bollimpelli, M. K. D. Scott, F. Wimmers, S. L. Burton, C. C. Labranche, C. Petitdemange, S. Gangadhara, T. M. Styles, C. F. Quarnstrom, K. A. Walter, T. J. Ketas, T. Legere, P. B. Jagadeesh Reddy, S. P. Kasturi, A. Tsai, B. Z. Yeung, S. Gupta, M. Tomai, J. Vasilakos, G. M. Shaw, C. Y. Kang, J. P. Moore, S. Subramaniam, P. Khatri, D. Montefiori, P. A. Kozlowski, C. A. Derdeyn, E. Hunter, D. Masopust, R. R. Amara, B. Pulendran, T cell-inducing vaccine durably prevents mucosal SHIV infection even with lower neutralizing antibody titers. *Nat Med* **26**, 932-940 (2020).
8. F. Martinon, S. Krishnan, G. Lenzen, R. Magne, E. Gomard, J. G. Guillet, J. P. Levy, P. Meulien, Induction of virus-specific cytotoxic T lymphocytes in vivo by liposome-entrapped mRNA. *Eur J Immunol* **23**, 1719-1722 (1993).
9. L. R. Baden, H. M. El Sahly, B. Essink, K. Kotloff, S. Frey, R. Novak, D. Diemert, S. A. Spector, N. Rouphael, C. B. Creech, J. McGettigan, S. Khetan, N. Segall, J. Solis, A. Brosz, C. Fierro, H. Schwartz, K. Neuzil, L. Corey, P. Gilbert, H. Janes, D. Follmann, M. Marovich, J. Mascola, L. Polakowski, J. Ledgerwood, B. S. Graham, H. Bennett, R. Pajon, C. Knightly, B. Leav, W. Deng, H. Zhou, S. Han, M. Ivarsson, J. Miller, T. Zaks, C. S. Group, Efficacy and Safety of the mRNA-1273 SARS-CoV-2 Vaccine. *N Engl J Med* **384**, 403-416 (2021).
10. L. A. Jackson, E. J. Anderson, N. G. Rouphael, P. C. Roberts, M. Makhene, R. N. Coler, M. P. McCullough, J. D. Chappell, M. R. Denison, L. J. Stevens, A. J. Pruijssers, A.

McDermott, B. Flach, N. A. Doria-Rose, K. S. Corbett, K. M. Morabito, S. O'Dell, S. D. Schmidt, P. A. Swanson, 2nd, M. Padilla, J. R. Mascola, K. M. Neuzil, H. Bennett, W. Sun, E. Peters, M. Makowski, J. Albert, K. Cross, W. Buchanan, R. Pikaart-Tautges, J. E. Ledgerwood, B. S. Graham, J. H. Beigel, R. N. A. S. G. m, An mRNA Vaccine against SARS-CoV-2 - Preliminary Report. *N Engl J Med* **383**, 1920-1931 (2020).

11. M. J. Mulligan, K. E. Lyke, N. Kitchin, J. Absalon, A. Gurtman, S. Lockhart, K. Neuzil, V. Raabe, R. Bailey, K. A. Swanson, P. Li, K. Koury, W. Kalina, D. Cooper, C. Fontes-Garfias, P. Y. Shi, O. Tureci, K. R. Tompkins, E. E. Walsh, R. Frenck, A. R. Falsey, P. R. Dormitzer, W. C. Gruber, U. Sahin, K. U. Jansen, Phase I/II study of COVID-19 RNA vaccine BNT162b1 in adults. *Nature* **586**, 589-593 (2020).
12. N. Dagan, N. Barda, E. Kepten, O. Miron, S. Perchik, M. A. Katz, M. A. Hernan, M. Lipsitch, B. Reis, R. D. Balicer, BNT162b2 mRNA Covid-19 Vaccine in a Nationwide Mass Vaccination Setting. *N Engl J Med* **384**, 1412-1423 (2021).
13. K. Sano, D. Bhavsar, G. Singh, D. Floda, K. Srivastava, C. Gleason, P. S. Group, J. M. Carreno, V. Simon, F. Krammer, SARS-CoV-2 vaccination induces mucosal antibody responses in previously infected individuals. *Nat Commun* **13**, 5135 (2022).
14. J. Declercq, E. Tobback, S. Vanhee, N. De Ruyck, S. Gerlo, P. Gevaert, L. Vandekerckhove, COVID-19 vaccination with BNT162b2 and ChAdOx1 vaccines has the potential to induce nasal neutralizing antibodies. *Allergy* **77**, 304-307 (2022).
15. F. Liew, S. Talwar, A. Cross, B. J. Willett, S. Scott, N. Logan, M. K. Siggins, D. Swieboda, J. K. Sidhu, C. Efstathiou, S. C. Moore, C. Davis, N. Mohamed, J. Nunag, C. King, A. A. R. Thompson, S. L. Rowland-Jones, A. B. Docherty, J. D. Chalmers, L. P. Ho, A. Horsley, B. Raman, K. Poinasamy, M. Marks, O. M. Kon, L. Howard, D. G. Wootton, S. Dunachie, J. K. Quint, R. A. Evans, L. V. Wain, S. Fontanella, T. I. de Silva, A. Ho, E. Harrison, J. K. Baillie, M. G. Semple, C. Brightling, R. S. Thwaites, L. Turtle, P. J. M. Openshaw, I. C. Investigators, P.-C. c. group, SARS-CoV-2-specific nasal IgA wanes 9 months after hospitalisation with COVID-19 and is not induced by subsequent vaccination. *EBioMedicine* **87**, 104402 (2023).
16. M. Guerrieri, B. Francavilla, D. Fiorelli, M. Nuccetelli, F. M. Passali, L. Coppeta, G. Somma, S. Bernardini, A. Magrini, S. Di Girolamo, Nasal and Salivary Mucosal Humoral Immune Response Elicited by mRNA BNT162b2 COVID-19 Vaccine Compared to SARS-CoV-2 Natural Infection. *Vaccines (Basel)* **9**, (2021).
17. J. Tang, C. Zeng, T. M. Cox, C. Li, Y. M. Son, I. S. Cheon, Y. Wu, S. Behl, J. J. Taylor, R. Chakaraborty, A. J. Johnson, D. N. Shiavo, J. P. Utz, J. S. Reisenauer, D. E. Midthun, J. J. Mullon, E. S. Edell, M. G. Alameh, L. Borish, W. G. Teague, M. H. Kaplan, D. Weissman, R. Kern, H. Hu, R. Vassallo, S. L. Liu, J. Sun, Respiratory mucosal immunity against SARS-CoV-2 after mRNA vaccination. *Sci Immunol* **7**, eadd4853 (2022).
18. S. Sheikh-Mohamed, B. Isho, G. Y. C. Chao, M. Zuo, C. Cohen, Y. Lustig, G. R. Nahass, R. E. Salomon-Shulman, G. Blacker, M. Fazel-Zarandi, B. Rathod, K. Colwill, A. Jamal, Z. Li, K. Q. de Launay, A. Takaoka, J. Garnham-Takaoka, A. Patel, C. Fahim, A. Paterson, A. X. Li, N. Haq, S. Barati, L. Gilbert, K. Green, M. Mozafarihashjin, P. Samaan, P. Budylowski, W. L. Siqueira, S. Mubareka, M. Ostrowski, J. M. Rini, O. L. Rojas, I. L. Weissman, M. C. Tal, A. McGeer, G. Regev-Yochay, S. Straus, A. C. Gingras, J. L. Gommerman, Systemic and mucosal IgA responses are variably induced in response to SARS-CoV-2 mRNA vaccination and are associated with protection against subsequent infection. *Mucosal Immunol* **15**, 799-808 (2022).

19. L. Azzi, D. Dalla Gasperina, G. Veronesi, M. Shallak, G. Ietto, D. Iovino, A. Baj, F. Gianfagna, V. Maurino, D. Focosi, F. Maggi, M. M. Ferrario, F. Dentali, G. Carcano, A. Tagliabue, L. S. Maffioli, R. S. Accolla, G. Forlani, Mucosal immune response in BNT162b2 COVID-19 vaccine recipients. *EBioMedicine* **75**, 103788 (2022).
20. G. Gorochov, J. Ropers, O. Launay, K. Dorgham, O. da Mata-Jardin, S. Lebbah, C. Durier, R. Bauer, A. Radenne, C. Desaint, L. V. Vieillard, C. Rekacewicz, M. Lachatre, B. Parfait, F. Batteux, P. Hupe, L. Ninove, M. Lefebvre, A. Conrad, B. Dussol, Z. Maakaroun-Vermesse, G. Melica, J. F. Nicolas, R. Verdon, J. J. Kiladjian, P. Loubet, C. Schmidt-Mutter, C. Duale, S. Ansart, E. Botelho-Nevers, J. D. Lelievre, X. de Lamballerie, M. P. Kieny, E. Tartour, S. Paul, Serum and Salivary IgG and IgA Response After COVID-19 Messenger RNA Vaccination. *JAMA Netw Open* **7**, e248051 (2024).
21. Y. J. Park, D. Pinto, A. C. Walls, Z. Liu, A. De Marco, F. Benigni, F. Zatta, C. Silacci-Fregni, J. Bassi, K. R. Sprouse, A. Addetia, J. E. Bowen, C. Stewart, M. Giurdanella, C. Saliba, B. Guarino, M. A. Schmid, N. M. Franko, J. K. Logue, H. V. Dang, K. Hauser, J. di Iulio, W. Rivera, G. Schnell, A. Rajesh, J. Zhou, N. Farhat, H. Kaiser, M. Montiel-Ruiz, J. Noack, F. A. Lempp, J. Janer, R. Abdelnabi, P. Maes, P. Ferrari, A. Ceschi, O. Giannini, G. D. de Melo, L. Kergoat, H. Bourhy, J. Neyts, L. Soriaga, L. A. Purcell, G. Snell, S. P. J. Whelan, A. Lanzavecchia, H. W. Virgin, L. Piccoli, H. Y. Chu, M. S. Pizzuto, D. Corti, D. Veesler, Imprinted antibody responses against SARS-CoV-2 Omicron sublineages. *Science* **378**, 619-627 (2022).
22. D. Planas, I. Staropoli, F. Porot, F. Guivel-Benhassine, L. Handala, M. Prot, W. H. Bolland, J. Puech, H. Pere, D. Veyer, A. Seve, E. Simon-Loriere, T. Bruel, T. Prazuck, K. Stefic, L. Hocqueloux, O. Schwartz, Duration of BA.5 neutralization in sera and nasal swabs from SARS-CoV-2 vaccinated individuals, with or without omicron breakthrough infection. *Med* **3**, 838-847 e833 (2022).
23. S. Terreri, E. Piano Mortari, M. R. Vinci, C. Russo, C. Alteri, C. Albano, F. Colavita, G. Gramigna, C. Agrati, G. Linardos, L. Coltella, L. Colagrossi, G. Deriu, M. Ciofi Degli Atti, C. Rizzo, M. Scarsella, R. Brugaletta, V. Camisa, A. Santoro, G. Roscilli, E. Pavoni, A. Muzi, N. Magnavita, R. Scutari, A. Villani, M. Raponi, F. Locatelli, C. F. Perno, S. Zaffina, R. Carsetti, Persistent B cell memory after SARS-CoV-2 vaccination is functional during breakthrough infections. *Cell Host Microbe* **30**, 400-408 e404 (2022).
24. P. Brandtzaeg, Secretory immunity with special reference to the oral cavity. *J Oral Microbiol* **5**, (2013).
25. S. A. Wellford, A. P. Moseman, K. Dao, K. E. Wright, A. Chen, J. E. Plevin, T. C. Liao, N. Mehta, E. A. Moseman, Mucosal plasma cells are required to protect the upper airway and brain from infection. *Immunity* **55**, 2118-2134 e2116 (2022).
26. C. W. Tan, W. N. Chia, X. Qin, P. Liu, M. I. Chen, C. Tiu, Z. Hu, V. C. Chen, B. E. Young, W. R. Sia, Y. J. Tan, R. Foo, Y. Yi, D. C. Lye, D. E. Anderson, L. F. Wang, A SARS-CoV-2 surrogate virus neutralization test based on antibody-mediated blockage of ACE2-spike protein-protein interaction. *Nat Biotechnol* **38**, 1073-1078 (2020).
27. A. Cagigi, M. Yu, B. Osterberg, J. Svensson, S. Falck-Jones, S. Vangeti, E. Ahlberg, L. Azizmohammadi, A. Warnqvist, R. Falck-Jones, P. C. Gubisch, M. Odemis, F. Ghafoor, M. Eisele, K. Lenart, M. Bell, N. Johansson, J. Albert, J. Salde, D. D. Pettie, M. P. Murphy, L. Carter, N. P. King, S. Ols, J. Normark, C. Ahlm, M. N. Forsell, A. Farnert, K. Lore, A. Smed-Sorensen, Airway antibodies emerge according to COVID-19 severity and wane rapidly but reappear after SARS-CoV-2 vaccination. *JCI Insight* **6**, (2021).

28. U. Marking, O. Bladh, S. Havervall, J. Svensson, N. Greilert-Norin, K. Aguilera, M. Kihlgren, A. C. Salomonsson, M. Mansson, R. Gallini, C. Kriegholm, P. Bacchus, S. Hober, M. Gordon, K. Blom, A. Smed-Sorensen, M. Aberg, J. Klingstrom, C. Thalin, 7-month duration of SARS-CoV-2 mucosal immunoglobulin-A responses and protection. *Lancet Infect Dis* **23**, 150-152 (2023).
29. O. Bladh, U. Marking, S. Havervall, N. G. Norin, K. Aguilera, S. Hober, A. Smed-Sorensen, M. Gordon, K. Blom, M. Aberg, J. Klingstrom, C. Thalin, Mucosal immune responses following a fourth SARS-CoV-2 vaccine dose. *Lancet Microbe* **4**, e488 (2023).
30. P. Brandtzaeg, H. Prydz, Direct evidence for an integrated function of J chain and secretory component in epithelial transport of immunoglobulins. *Nature* **311**, 71-73 (1984).
31. F. E. Johansen, R. Braathen, P. Brandtzaeg, Role of J chain in secretory immunoglobulin formation. *Scand J Immunol* **52**, 240-248 (2000).
32. Z. Wang, F. Muecksch, D. Schaefer-Babajew, S. Finkin, C. Viant, C. Gaebler, H. H. Hoffmann, C. O. Barnes, M. Cipolla, V. Ramos, T. Y. Oliveira, A. Cho, F. Schmidt, J. Da Silva, E. Bednarski, L. Aguado, J. Yee, M. Daga, M. Turroja, K. G. Millard, M. Jankovic, A. Gazumyan, Z. Zhao, C. M. Rice, P. D. Bieniasz, M. Caskey, T. Hatziioannou, M. C. Nussenzweig, Naturally enhanced neutralizing breadth against SARS-CoV-2 one year after infection. *Nature* **595**, 426-431 (2021).
33. J. S. Turner, J. A. O'Halloran, E. Kalaidina, W. Kim, A. J. Schmitz, J. Q. Zhou, T. Lei, M. Thapa, R. E. Chen, J. B. Case, F. Amanat, A. M. Rauseo, A. Haile, X. Xie, M. K. Klebert, T. Suessen, W. D. Middleton, P. Y. Shi, F. Krammer, S. A. Teefey, M. S. Diamond, R. M. Presti, A. H. Ellebedy, SARS-CoV-2 mRNA vaccines induce persistent human germinal centre responses. *Nature* **596**, 109-113 (2021).
34. W. F. Garcia-Beltran, K. J. St Denis, A. Hoelzemer, E. C. Lam, A. D. Nitido, M. L. Sheehan, C. Berrios, O. Ofoman, C. C. Chang, B. M. Hauser, J. Feldman, A. L. Roederer, D. J. Gregory, M. C. Poznansky, A. G. Schmidt, A. J. Iafrate, V. Naranbhai, A. B. Balazs, mRNA-based COVID-19 vaccine boosters induce neutralizing immunity against SARS-CoV-2 Omicron variant. *Cell* **185**, 457-466 e454 (2022).
35. M. Hoffmann, N. Kruger, S. Schulz, A. Cossmann, C. Rocha, A. Kempf, I. Nehlmeier, L. Graichen, A. S. Moldenhauer, M. S. Winkler, M. Lier, A. Dopfer-Jablonka, H. M. Jack, G. M. N. Behrens, S. Pohlmann, The Omicron variant is highly resistant against antibody-mediated neutralization: Implications for control of the COVID-19 pandemic. *Cell* **185**, 447-456 e411 (2022).
36. Z. Wang, J. C. C. Lorenzi, F. Muecksch, S. Finkin, C. Viant, C. Gaebler, M. Cipolla, H. H. Hoffmann, T. Y. Oliveira, D. A. Oren, V. Ramos, L. Nogueira, E. Michailidis, D. F. Robbiani, A. Gazumyan, C. M. Rice, T. Hatziioannou, P. D. Bieniasz, M. Caskey, M. C. Nussenzweig, Enhanced SARS-CoV-2 neutralization by dimeric IgA. *Sci Transl Med* **13**, (2021).
37. D. Follmann, H. E. Janes, O. D. Buhule, H. Zhou, B. Girard, K. Marks, K. Kotloff, M. Desjardins, L. Corey, K. M. Neuzil, J. M. Miller, H. M. El Sahly, L. R. Baden, Antinucleocapsid Antibodies After SARS-CoV-2 Infection in the Blinded Phase of the Randomized, Placebo-Controlled mRNA-1273 COVID-19 Vaccine Efficacy Clinical Trial. *Ann Intern Med* **175**, 1258-1265 (2022).
38. D. H. Barouch, Covid-19 Vaccines - Immunity, Variants, Boosters. *N Engl J Med* **387**, 1011-1020 (2022).

39. D. Y. Lin, Y. Gu, B. Wheeler, H. Young, S. Holloway, S. K. Sunny, Z. Moore, D. Zeng, Effectiveness of Covid-19 Vaccines over a 9-Month Period in North Carolina. *N Engl J Med* **386**, 933-941 (2022).
40. A. Britton, K. E. Fleming-Dutra, N. Shang, Z. R. Smith, T. Dorji, G. Derado, E. K. Accorsi, U. A. Ajani, J. Miller, S. J. Schrag, J. R. Verani, Association of COVID-19 Vaccination With Symptomatic SARS-CoV-2 Infection by Time Since Vaccination and Delta Variant Predominance. *JAMA* **327**, 1032-1041 (2022).
41. D. S. Khoury, D. Cromer, A. Reynaldi, T. E. Schlub, A. K. Wheatley, J. A. Juno, K. Subbarao, S. J. Kent, J. A. Triccas, M. P. Davenport, Neutralizing antibody levels are highly predictive of immune protection from symptomatic SARS-CoV-2 infection. *Nat Med* **27**, 1205-1211 (2021).
42. P. B. Gilbert, D. C. Montefiori, A. B. McDermott, Y. Fong, D. Benkeser, W. Deng, H. Zhou, C. R. Houchens, K. Martins, L. Jayashankar, F. Castellino, B. Flach, B. C. Lin, S. O'Connell, C. McDanal, A. Eaton, M. Sarzotti-Kelsoe, Y. Lu, C. Yu, B. Borate, L. W. P. van der Laan, N. S. Hejazi, C. Huynh, J. Miller, H. M. El Sahly, L. R. Baden, M. Baron, L. De La Cruz, C. Gay, S. Kalams, C. F. Kelley, M. P. Andrasik, J. G. Kublin, L. Corey, K. M. Neuzil, L. N. Carpp, R. Pajon, D. Follmann, R. O. Donis, R. A. Koup, s. Immune Assays Team section, I. T. s. s. Moderna, s. Coronavirus Vaccine Prevention Network /Coronavirus Efficacy Team section, V. P. N. B. T. s. s. United States Government /Co, Immune correlates analysis of the mRNA-1273 COVID-19 vaccine efficacy clinical trial. *Science* **375**, 43-50 (2022).
43. A. Y. Collier, J. Yu, K. McMahan, J. Liu, A. Chandrashekar, J. S. Maron, C. Atyeo, D. R. Martinez, J. L. Ansel, R. Aguayo, M. Rowe, C. Jacob-Dolan, D. Sellers, J. Barrett, K. Ahmad, T. Anioke, H. VanWyk, S. Gardner, O. Powers, E. A. Bondzie, H. Wan, R. S. Baric, G. Alter, M. R. Hacker, D. H. Barouch, Differential Kinetics of Immune Responses Elicited by Covid-19 Vaccines. *N Engl J Med* **385**, 2010-2012 (2021).
44. A. Pegu, S. E. O'Connell, S. D. Schmidt, S. O'Dell, C. A. Talana, L. Lai, J. Albert, E. Anderson, H. Bennett, K. S. Corbett, B. Flach, L. Jackson, B. Leav, J. E. Ledgerwood, C. J. Luke, M. Makowski, M. C. Nason, P. C. Roberts, M. Roederer, P. A. Rebolledo, C. A. Rostad, N. G. Rouphael, W. Shi, L. Wang, A. T. Widge, E. S. Yang, R. N. A. S. G. s. s. m, J. H. Beigel, B. S. Graham, J. R. Mascola, M. S. Suthar, A. B. McDermott, N. A. Doria-Rose, J. Arega, J. H. Beigel, W. Buchanan, M. Elsafy, B. Hoang, R. Lampley, A. Kolhekar, H. Koo, C. Luke, M. Makhene, S. Nayak, R. Pikaart-Tautges, P. C. Roberts, J. Russell, E. Sindall, J. Albert, P. Kunwar, M. Makowski, E. J. Anderson, A. Bechnak, M. Bower, A. F. Camacho-Gonzalez, M. Collins, A. Drobeniuc, V. V. Edara, S. Edupuganti, K. Floyd, T. Gibson, C. M. G. Ackerley, B. Johnson, S. Kamidani, C. Kao, C. Kelley, L. Lai, H. Macenczak, M. P. McCullough, E. Peters, V. K. Phadke, P. A. Rebolledo, C. A. Rostad, N. Rouphael, E. Scherer, A. Sherman, K. Stephens, M. S. Suthar, M. Teherani, J. Traenkner, J. Winston, I. Yildirim, L. Barr, J. Benoit, B. Carste, J. Choe, M. Dunstan, R. Erolin, J. Ffitch, C. Fields, L. A. Jackson, E. Kiniry, S. Lasicka, S. Lee, M. Nguyen, S. Pimienta, J. Suyehira, M. Witte, H. Bennett, N. E. Altaras, A. Carfi, M. Hurley, B. Leav, R. Pajon, W. Sun, T. Zaks, R. N. Coler, S. E. Larsen, K. M. Neuzil, L. C. Lindesmith, D. R. Martinez, J. Munt, M. Mallory, C. Edwards, R. S. Baric, N. M. Berkowitz, E. A. Boritz, K. Carlton, K. S. Corbett, P. Costner, A. Creanga, N. A. Doria-Rose, D. C. Douek, B. Flach, M. Gaudinski, I. Gordon, B. S. Graham, L. Holman, J. E. Ledgerwood, K. Leung, B. C. Lin, M. K. Louder, J. R. Mascola, A. B. McDermott, K. M. Morabito, L.

Novik, S. O'Connell, S. O'Dell, M. Padilla, A. Pegu, S. D. Schmidt, W. Shi, P. A. Swanson, 2nd, C. A. Talana, L. Wang, A. T. Widge, E. S. Yang, Y. Zhang, J. D. Chappell, M. R. Denison, T. Hughes, X. Lu, A. J. Pruijssers, L. J. Stevens, C. M. Posavad, M. Gale, Jr., V. Menachery, P. Y. Shi, Durability of mRNA-1273 vaccine-induced antibodies against SARS-CoV-2 variants. *Science* **373**, 1372-1377 (2021).

45. E. G. Levin, Y. Lustig, C. Cohen, R. Fluss, V. Indenbaum, S. Amit, R. Doolman, K. Asraf, E. Mendelson, A. Ziv, C. Rubin, L. Freedman, Y. Kreiss, G. Regev-Yochay, Waning Immune Humoral Response to BNT162b2 Covid-19 Vaccine over 6 Months. *N Engl J Med* **385**, e84 (2021).
46. A. J. Macpherson, K. D. McCoy, F. E. Johansen, P. Brandtzaeg, The immune geography of IgA induction and function. *Mucosal Immunol* **1**, 11-22 (2008).
47. B. Johansson-Lindbom, W. W. Agace, Generation of gut-homing T cells and their localization to the small intestinal mucosa. *Immunol Rev* **215**, 226-242 (2007).
48. E. C. Lavelle, R. W. Ward, Mucosal vaccines - fortifying the frontiers. *Nat Rev Immunol* **22**, 236-250 (2022).
49. H. Brussow, Do we need nasal vaccines against COVID 19 to suppress the transmission of infections? *Microb Biotechnol* **16**, 3-14 (2023).
50. F. Zhu, C. Zhuang, K. Chu, L. Zhang, H. Zhao, S. Huang, Y. Su, H. Lin, C. Yang, H. Jiang, X. Zang, D. Liu, H. Pan, Y. Hu, X. Liu, Q. Chen, Q. Song, J. Quan, Z. Huang, G. Zhong, J. Chen, J. Han, H. Sun, L. Cui, J. Li, Y. Chen, T. Zhang, X. Ye, C. Li, T. Wu, J. Zhang, N. S. Xia, Safety and immunogenicity of a live-attenuated influenza virus vector-based intranasal SARS-CoV-2 vaccine in adults: randomised, double-blind, placebo-controlled, phase 1 and 2 trials. *Lancet Respir Med* **10**, 749-760 (2022).
51. M. Madhavan, A. J. Ritchie, J. Aboagye, D. Jenkin, S. Provstgaad-Morys, I. Tarbet, D. Woods, S. Davies, M. Baker, A. Platt, A. Flaxman, H. Smith, S. Belij-Rammerstorfer, D. Wilkins, E. J. Kelly, T. Villafana, J. A. Green, I. Poulton, T. Lambe, A. V. S. Hill, K. J. Ewer, A. D. Douglas, Tolerability and immunogenicity of an intranasally-administered adenovirus-vectored COVID-19 vaccine: An open-label partially-randomised ascending dose phase I trial. *EBioMedicine* **85**, 104298 (2022).
52. . (https://ir.altimmune.com/news-releases/news-release-details/altimmune-announces-update-adcovidtm-phase-1-clinical-trial, 2021).
53. A. Suberi, M. K. Grun, T. Mao, B. Israelow, M. Reschke, J. Grundler, L. Akhtar, T. Lee, K. Shin, A. S. Piotrowski-Daspit, R. J. Homer, A. Iwasaki, H. W. Suh, W. M. Saltzman, Polymer nanoparticles deliver mRNA to the lung for mucosal vaccination. *Sci Transl Med* **15**, eabq0603 (2023).
54. J. D. Clements, E. B. Norton, The Mucosal Vaccine Adjuvant LT(R192G/L211A) or dmLT. *mSphere* **3**, (2018).
55. F. Su, G. B. Patel, S. Hu, W. Chen, Induction of mucosal immunity through systemic immunization: Phantom or reality? *Hum Vaccin Immunother* **12**, 1070-1079 (2016).
56. P. Gevaert, C. Bachert, G. Holtappels, C. P. Novo, J. Van der Heyden, L. Fransen, S. Depraetere, H. Walter, P. van Cauwenberge, J. Tavernier, Enhanced soluble interleukin-5 receptor alpha expression in nasal polyposis. *Allergy* **58**, 371-379 (2003).
57. M. Berings, S. Arasi, N. De Ruyck, S. Perna, Y. Resch, C. Lupinek, K. W. Chen, S. Vrtala, G. B. Pajno, C. Bachert, B. N. Lambrecht, M. Dullaers, R. Valenta, P. M. Matricardi, P. Gevaert, Reliable mite-specific IgE testing in nasal secretions by means of allergen microarray. *J Allergy Clin Immunol* **140**, 301-303 e308 (2017).

58. D. Wrapp, N. Wang, K. S. Corbett, J. A. Goldsmith, C. L. Hsieh, O. Abiona, B. S. Graham, J. S. McLellan, Cryo-EM structure of the 2019-nCoV spike in the prefusion conformation. *Science* **367**, 1260-1263 (2020).

Acknowledgments

We thank all study participants for their participation in our study, and all people involved in the sample collection of our prospective longitudinal study. We also thank the VIB-core facilities for their technical assistance, in particular the VIB flow core facility, VIB protein core facility, and VIB animal house facility.

Funding:

This work was supported by Fonds Wetenschappelijk Onderzoek Vlaanderen PhD Fellowship Grants 3F015119 (to J.D.), 3S035019 (to S.V.N.), 11PNN24N (to N.G.), and 11D9623N (to I.L.); Fonds Wetenschappelijk Onderzoek Vlaanderen Senior Postdoc Fellowship Grant 1244321N (to S.V.); the Collen-Francqui Research Professor Mandate (to L.V.); European Research Council Advanced Grant ERC -2017-ADG- 789384 (to B.N.L.); FWO and F.R.S.-FNRS Excellence of Science (EOS) UHEAD grant G0G2318N (to B.N.L.) and BENEFICIARIES consortium grant 3G0H1222 (to B.N.L.); Concerted Research Action grant of Ghent University BOF17/GOOA/028: 01G010C9 (to B.N.L.); Special Research Fund of Ghent University Methusalem grant 01GA2817: 01M01521 (to B.N.L.); VIB Grand Challenge grants M901BALA-GCP-COVID-19-SARPAC TRIAL and M902BALA-GCP-COVID-19-IL6-IL1 TRIAL (to B.N.L.); Fonds Wetenschappelijk Onderzoek Vlaanderen COVID-19 Grant G0G4520N (to L.V.); Fonds Wetenschappelijk Onderzoek Vlaanderen grant 1.8.020.09.N.00 (to L.V.); Fonds Wetenschappelijk Onderzoek Vlaanderen project grant G0A7422N (to P.G. and S.V.);Bijzonder Onderzoeksfonds Fonds Ghent University grant 01C04620 (to L.V.); and EOS joint program of Fonds de la Recherce Scientifice and Fonds Wetenschappelijk Onderzoek Vlaanderen G0H7322N EOS ID: 40007527 (to X.S.).

Author contributions:

JD, SG, PG, LV, and SV conceptualized the study. JD, SVN, NDR, GH, IL, KR, BS, and KS developed the methodology. JD, SVN, NDR, GH, LD, ET, IL, and KS performed the experiments.

JD and SV visualized the data. PG, SV, SH, LV, BNL, and XS acquired funding. LD, ET, and NDR performed project administration. SG, BNL, PG, LV, SV, and XS supervised the study. JD wrote the original draft of the manuscript. JD, PG, SV, SG, LV, BNL, and XS revised the original draft and contributed to the finalization of the manuscript. All authors reviewed and edited the manuscript.

Competing interests:

BNL received consulting fees from Sanofi and GSK and holds stock options from ArgenX. PG has served as an advisor or speaker or has received research support from 3NT, Ablynx, ALK, ArgenX, AstraZeneca, Bekaert Textiles, Genentech, GSK, Hall Allergy, Medtronic, Novartis, Regeneron, Roche, Sanofi-Genzyme, Stallergenes-Greer, Teva, and Thermo Fisher. LV received grants from Gilead Sciences. XS is a scientific co-founder of Exevir Bio. The other authors declare that they have no competing interests.

Data and materials availability:

All data associated with this study are in the paper or supplementary materials. Patient samples and information cannot be shared without additional patient consent. For questions regarding patient samples the Health, innovation and research institute of the University Hospital Ghent should be contacted (hiruz@uzgent.be) as well as Prof. Dr. Linos Vandekerckhove (Linos.Vandekerckhove@UGent.be). All other correspondence and requests can be addressed to Prof. Dr. Stijn Vanhee (Stijn.vanhee@ugent.be).

Figures

Figure 1. Repeated mRNA vaccination induces SARS-CoV_2 NAbs in the nasal mucosa.

(**A**) Schematic representation of study design and study flow chart. (**B**) Violin plots depicting NAb titers in serum (red) and nasal secretions (blue) at baseline and at 2 to 4 weeks and 6 months after primary and booster vaccinations in study participants receiving an mRNA-based vaccine as both primary and booster vaccination. Lines in the violin plots show median and quartiles, dotted line represents cut-off for neutralization based on pre-COVID-19 samples. Significance was determined by Kruskal-Wallis test with Dunn's test for multiple testing. (**C**) Dot plots displaying correlation between serum and nasal NAb titers shown in (B) at 2 to 4 weeks after primary mRNA vaccination and after 2 to 4 weeks after booster mRNA vaccination in participants vaccinated with BNT162b2 for their primary series. Lines represent simple linear regression with 95% CIs. The correlation and significance were tested by a two-tailed Spearman correlation test. (**D and E**) Violin plots depicting NAb titers in nasal secretions after primary (D) and booster (E) vaccination, according to primary vaccination with either mRNA-based (blue; data shown in (B)) or AVV-based (gray) vaccines. Both groups received an mRNA booster vaccine. Lines in the violin plots show median and quartiles, dotted line represents cut-off for neutralization based on pre-COVID-19 samples. Significance was determined by Mann-Whitney U test. Significance values are indicated by ***$p < 0.001$ and ****$p < 0.0001$; ns, not significant. For (B), significance values for comparisons between prior vaccination with any other timepoint are indicated by ####$p < 0.0001$. LOD, limit of detection.

Figure 2. Prior COVID-19 enhances mucosal neutralizing antibody titers upon vaccination.

(**A**) Violin plots depict NAb titers in serum (red) and nasal secretions (blue) at baseline and at 2 to 4 weeks and 6 months after primary mRNA vaccination. Participants are subdivided based on the presence of serum anti-N IgG prior to vaccination. Participants exhibiting seroconversion of anti-N IgG during the 6-month time course after primary vaccination were excluded from this analysis. (**B**) Violin plots depict NAb titers in serum (red) and nasal secretions (blue) at 2 to 4 weeks and 6 months after booster mRNA vaccination in individuals receiving primary mRNA vaccination. Participants are subdivided based on the presence of serum anti-N IgG at any timepoint prior to booster vaccination. Participants exhibiting seroconversion of anti-N IgG during the 6-month time course after booster vaccination were excluded from this analysis. (**C**) Violin plots depict NAb

titers in serum (red) and nasal secretions (blue) at 2 to 4 weeks after booster mRNA vaccination in participants receiving primary AVV-based vaccination and mRNA-based booster vaccination. Participants are subdivided based on the presence of serum anti-N IgG at any timepoint prior to booster vaccination. Participants exhibiting seroconversion of anti-N IgG during the 6-month time course after booster vaccination were excluded from this analysis. Lines in the violin plots show median and quartiles, dotted line represents cut-off for neutralization based on pre-COVID-19 samples. Significance was determined by Mann-Whitney U tests with Holm-Sidak method for multiple testing for (A) and (B). Significance values are indicated by *p < 0.05, **p < 0.01, ***p < 0.001, and ****p < 0.0001; ns, not significant.

Figure 3. Vaccine-induced SARS-CoV-2 NAbs antibodies are of IgG and IgA isotypes in both serum and nasal secretions.

(**A and B**) Anti-S1 IgG (A) and IgA (B) titers in serum (red) and nasal secretions (blue) at baseline and at 2 to 4 weeks and 6 months after primary and booster mRNA vaccination. (**C and D**) Anti-S1 IgG (C) and IgA (D) titers in serum (red) and nasal secretions (blue) at 2 to 4 weeks after mRNA booster vaccination, according to primary vaccination with either mRNA- (red or blue, data shown in (A and B) or AVV-based (gray) vaccines. (**E and F**) Anti-S1 IgG (E) and IgA (F) titers in serum (red) and nasal secretions (blue) at 2 to 4 weeks post primary mRNA vaccination. Participants are subdivided based on the presence of serum anti-N IgG prior to vaccination. Participants exhibiting seroconversion of anti-N IgG during the 6-month time course after primary vaccination were excluded from this analysis. (**G and H**) Anti-S1 IgG (G) and IgA (H) titers in serum (red) and nasal secretions (blue) at 2 to 4 weeks post booster mRNA vaccination in participants receiving mRNA- (red or blue) or AAV-based (gray) vaccines as primary vaccination. Participants are subdivided based on the presence of serum anti-N IgG prior to booster vaccination. Participants exhibiting seroconversion of anti-N IgG during the 6-month time course after booster vaccination were excluded from this analysis. All data are represented by violin plots with lines depicting the median and quartiles, and the dotted line representing the cut-off for neutralization based on pre-COVID-19 samples. Significance was determined by Mann-Whitney U test with Holm-Sidak method for multiple testing for (A) and (B). Significance values are indicated by *p < 0.05, **p < 0.01, and ***p < 0.001; ns, not significant. For (A) and (B) significance values for

comparisons between prior vaccination with any other timepoint are indicated by #p < 0.05, ##p < 0.01, and #### p < 0.0001. AU, arbitrary units.

Figure 4. Repeated mRNA vaccination induces serum and BAL SARS-CoV-2 NAbs in mice in the absence of detectable antibody producing cells in the respiratory mucosa.

(A) Schematic overview of immunizations and analysis timepoints. Mice were repeatedly immunized intramuscularly (right leg) with the BNT162b2 vaccine at the indicated timepoints. **(B to D)** Virus NAb titers (B), S-specific IgG (C), and S-specific IgA (D) in serum (red) and BAL fluid (BALf, blue) of mice that received no (n=9), 1 (n=5), 2 (n=5), 3 (n=5) or 4 (n=5) mRNA vaccinations. Mice were euthanized 3 weeks after the last immunization. Dotted lines represent the OD value of blanks. Data are representative of 2 independent experiments. Ctrl, control. **(E)** Representative flow cytometric gating for identification of S-specific B cells and GC B cells. **(F)** Number of S-specific B cells, the fraction of GC B cells among the S-specific B cells, and the number of S-specific PBPCs in the draining iLN, spleen, non-draining mLN, and lung of mice 4 times vaccinated (n=5) and control mice (n=5). Mice were euthanized 1 week after the fourth immunization. Data are representative of 2 independent experiments. **(G)** Representative flow plots of S-specific B cells and PBPCs in iLN, spleen, bone marrow, mLN, and lungs of vaccinated mice at 7 days after the fourth immunization. **(H)** Quantification of S-specific PBPCs in the bone marrow of mice that received no (n=9), 1 (n=5), 2 (n=5), 3 (n=5) or 4 (n=5) mRNA vaccinations. Mice were euthanized 21 days after the last immunization. Data are representative of 2 independent experiments. **(I and J)** Representative images (left) and quantification (right) of ELISPOTs to detect S-specific IgG-secreting cells (I) and IgA-secreting cells (J) in bone marrow and lungs from naïve (n=4) and 4 times vaccinated (n=10) mice. Mice were euthanized 21 days after the last immunization. Lung single cell suspensions were magnetically depleted of IV labeled cells (CD45 biotin). Data are pooled from 2 independent experiments. **(K)** Schematic overview of immunizations and serum and BALf harvests. Twice vaccinated mice were euthanized 21 days after the last immunization and serum was harvested. The serum was adoptively transferred in naïve recipients. **(L)** Virus NAb titers in serum (red) and BALf (blue) of naïve mice that received serum from control (Ctrl) or twice vaccinated (Vac) mice. Mice were euthanized 20 hours after serum transfer. Data are pooled from 2 independent experiments. All data are represented by bar graphs depicting the median. Statistical significance was tested by Kruskal-Wallis test with Dunn's

correction for multiple testing for (B), (C), (D), and (H) and Mann-Whitney U test for (F), (I), (J), and (L). Significance values are indicated by *p < 0.05, **p < 0.01, ***p < 0.001, and ****p < 0.0001; ns, not significant.

Figure 1

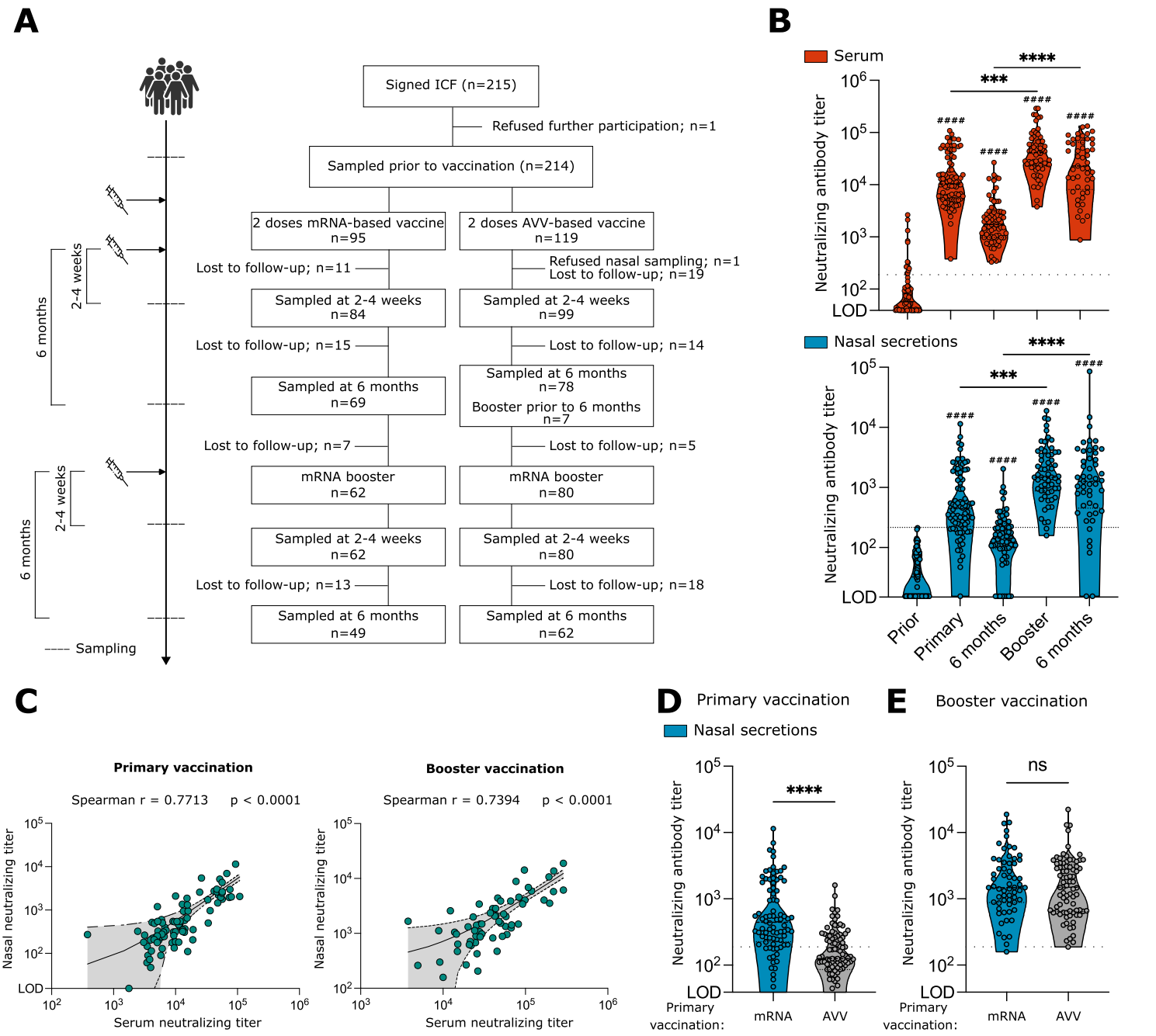
A
Signed ICF (n=215)
Refused further participation; n=1
Sampled prior to vaccination (n=214)
2 doses mRNA-based vaccine n=95
2 doses AVV-based vaccine n=119
Lost to follow-up; n=11
Refused nasal sampling; n=1
Lost to follow-up; n=19
Sampled at 2-4 weeks n=84
Sampled at 2-4 weeks n=99
Lost to follow-up; n=15
Lost to follow-up; n=14
Sampled at 6 months n=69
Sampled at 6 months n=78
Booster prior to 6 months n=7
Lost to follow-up; n=7
Lost to follow-up; n=5
mRNA booster n=62
mRNA booster n=80
Sampled at 2-4 weeks n=62
Sampled at 2-4 weeks n=80
Lost to follow-up; n=13
Lost to follow-up; n=18
Sampled at 6 months n=49
Sampled at 6 months n=62
2-4 weeks
6 months
2-4 weeks
6 months
Sampling
B
Serum
Nasal secretions
Neutralizing antibody titer
LOD
Prior
Primary
6 months
Booster
6 months
C
Primary vaccination
Spearman r = 0.7713 p < 0.0001
Booster vaccination
Spearman r = 0.7394 p < 0.0001
Nasal neutralizing titer
Serum neutralizing titer
LOD
D
Primary vaccination
Nasal secretions
Neutralizing antibody titer
Primary vaccination:
mRNA
AVV
E
Booster vaccination
ns
Neutralizing antibody titer
Primary vaccination:
mRNA
AVV

Figure 2

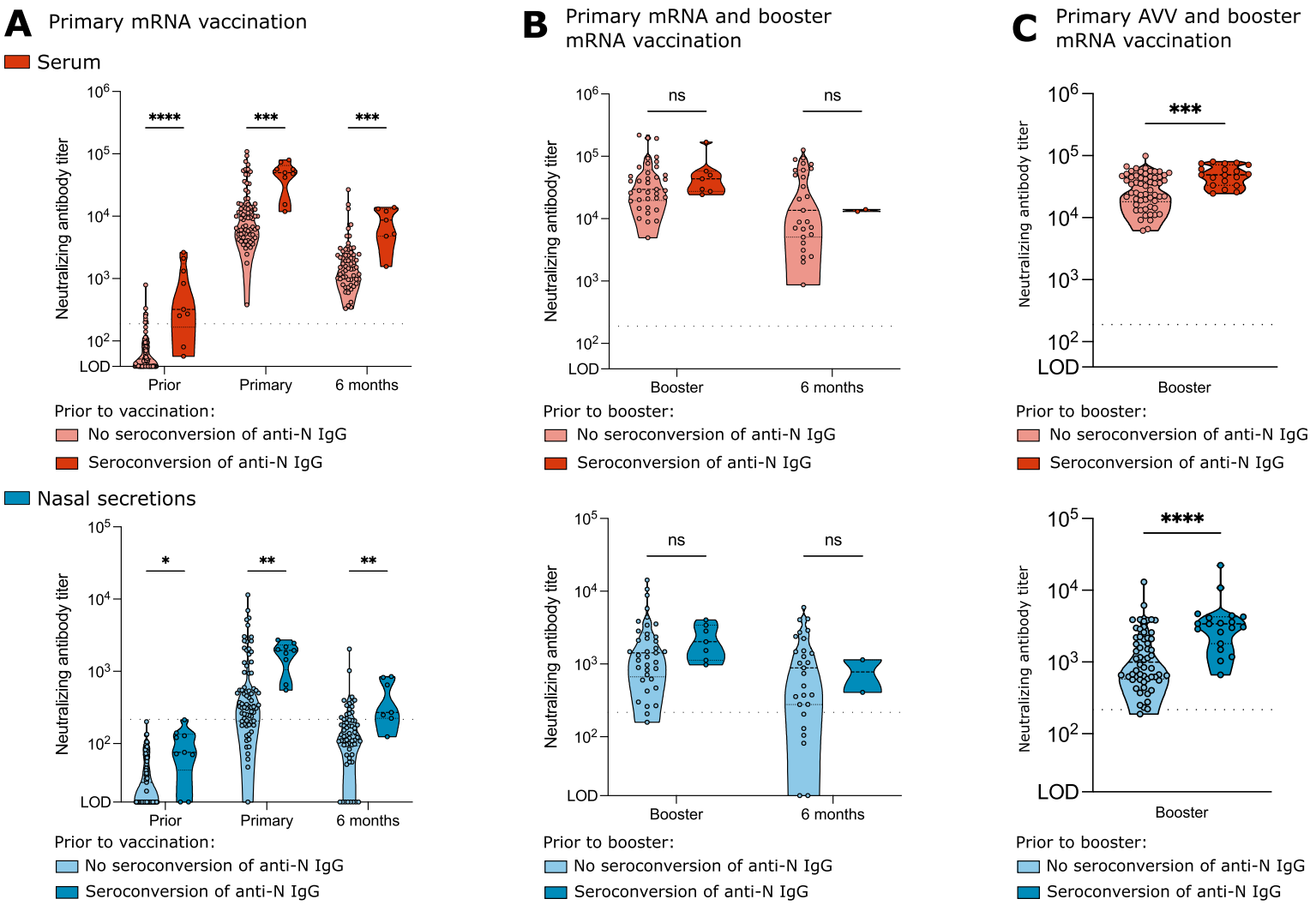
A
Primary mRNA vaccination
Serum
Neutralizing antibody titer
10^6
10^5
10^4
10^3
10^2
LOD
****
***
***
Prior
Primary
6 months
Prior to vaccination:
No seroconversion of anti-N IgG
Seroconversion of anti-N IgG
Nasal secretions
Neutralizing antibody titer
10^5
10^4
10^3
10^2
LOD
*
**
**
Prior
Primary
6 months
Prior to vaccination:
No seroconversion of anti-N IgG
Seroconversion of anti-N IgG
B
Primary mRNA and booster mRNA vaccination
Neutralizing antibody titer
10^6
10^5
10^4
10^3
10^2
LOD
ns
ns
Booster
6 months
Prior to booster:
No seroconversion of anti-N IgG
Seroconversion of anti-N IgG
Neutralizing antibody titer
10^5
10^4
10^3
10^2
LOD
ns
ns
Booster
6 months
Prior to booster:
No seroconversion of anti-N IgG
Seroconversion of anti-N IgG
C
Primary AVV and booster mRNA vaccination
Neutralizing antibody titer
10^6
10^5
10^4
10^3
10^2
LOD
***
Booster
Prior to booster:
No seroconversion of anti-N IgG
Seroconversion of anti-N IgG
Neutralizing antibody titer
10^5
10^4
10^3
10^2
LOD
****
Booster
Prior to booster:
No seroconversion of anti-N IgG
Seroconversion of anti-N IgG

Figure 3

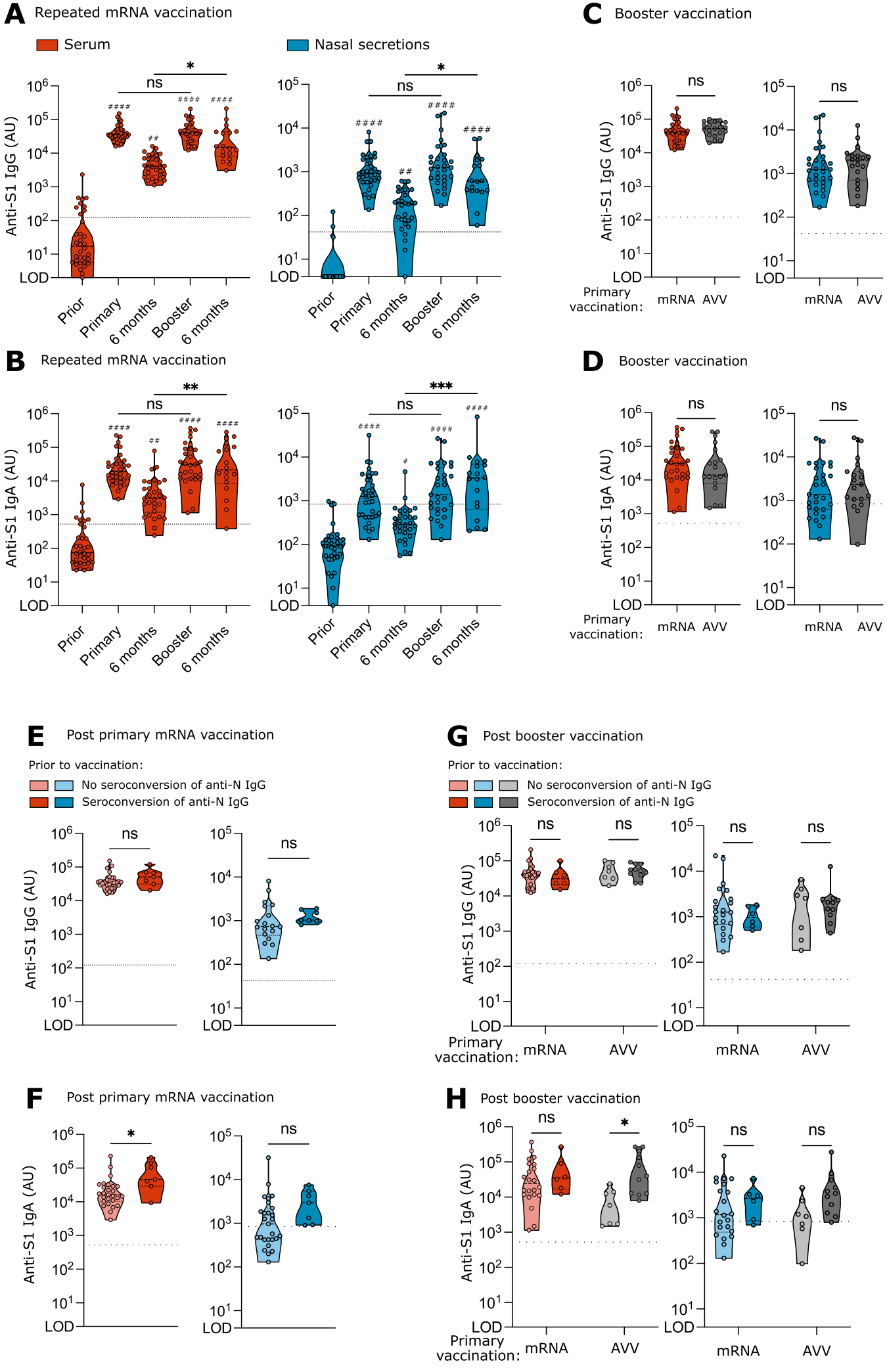
A
Repeated mRNA vaccination
Serum
Nasal secretions
Anti-S1 IgG (AU)
LOD
Prior
Primary
6 months
Booster
6 months
B
Repeated mRNA vaccination
Anti-S1 IgA (AU)
C
Booster vaccination
Primary vaccination:
mRNA
AVV
D
Booster vaccination
E
Post primary mRNA vaccination
Prior to vaccination:
No seroconversion of anti-N IgG
Seroconversion of anti-N IgG
F
Post primary mRNA vaccination
G
Post booster vaccination
H
Post booster vaccination
ns

Figure 4

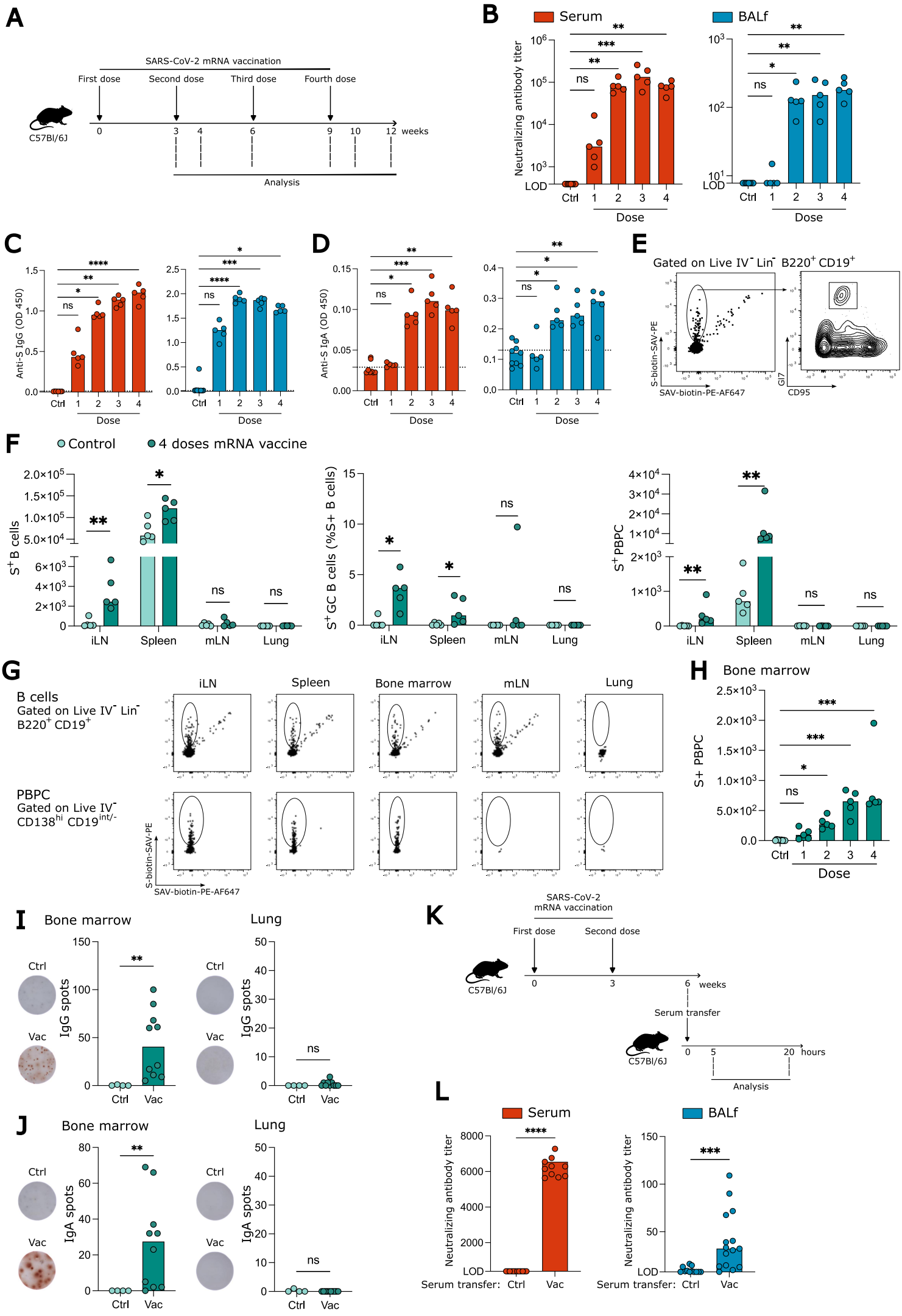
A
SARS-CoV-2 mRNA vaccination
First dose
Second dose
Third dose
Fourth dose
C57Bl/6J
0
3
4
6
9
10
12
weeks
Analysis
B
Serum
BALf
Neutralizing antibody titer
LOD
Ctrl
Dose
C
Anti-S IgG (OD 450)
Anti-S IgA (OD 450)
D
E
Gated on Live IV- Lin- B220+ CD19+
S-biotin-SAV-PE
SAV-biotin-PE-AF647
GI7
CD95
F
Control
4 doses mRNA vaccine
S+ B cells
S+ GC B cells (%S+ B cells)
S+ PBPC
iLN
Spleen
mLN
Lung
G
B cells
Gated on Live IV- Lin-
B220+ CD19+
PBPC
Gated on Live IV-
CD138hi CD19int/-
Bone marrow
H
I
IgG spots
Ctrl
Vac
J
IgA spots
K
SARS-CoV-2
mRNA vaccination
First dose
Second dose
Serum transfer
hours
Analysis
L
Serum transfer: Ctrl
Serum transfer: Vac

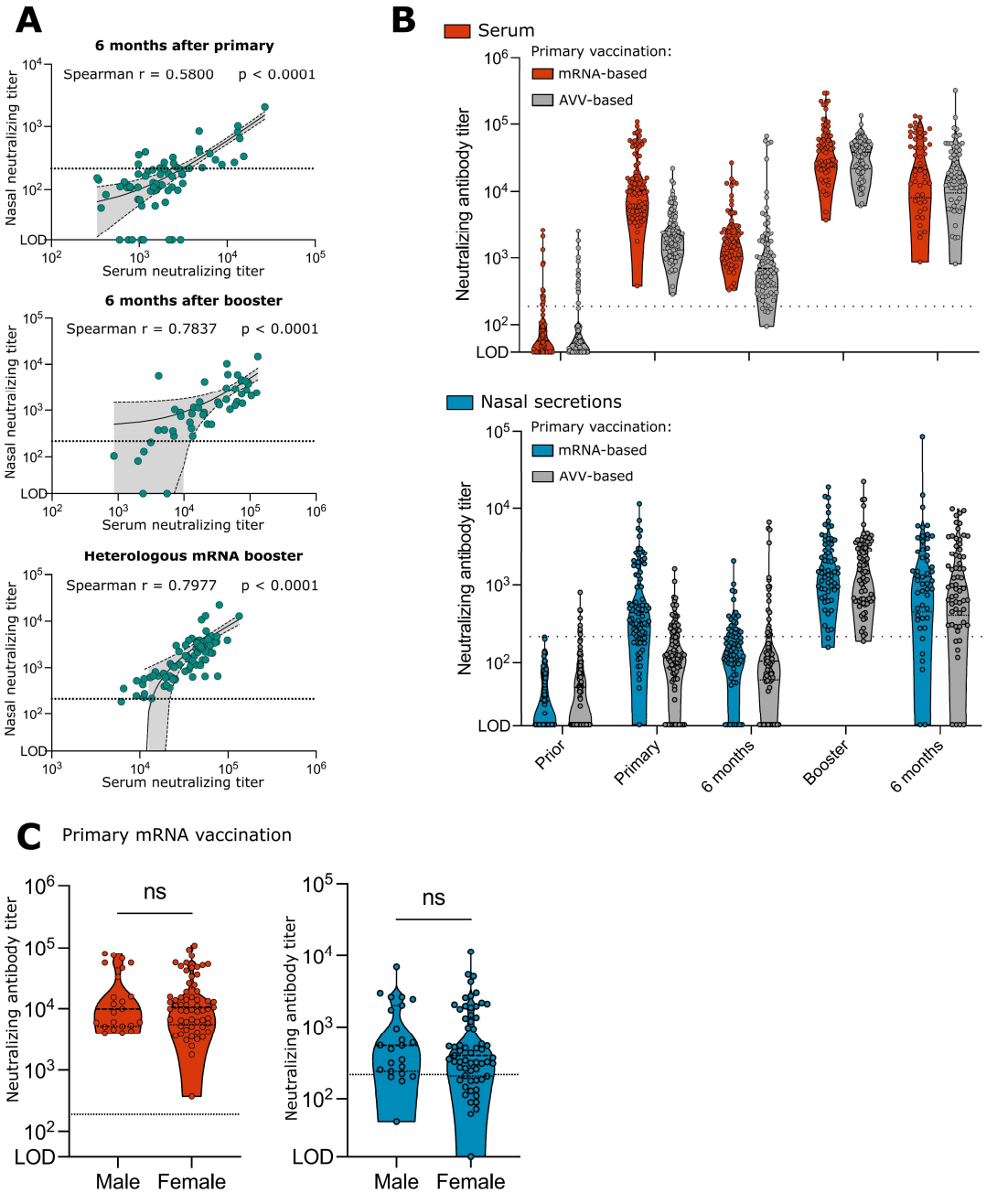

Fig. S1. Serum and nasal severe acute respiratory syndrome coronavirus 2 (SARS-CoV-2) neutralizing antibodies (NAb) upon mRNA- and adenovirus vector (AVV)-based vaccination.

(A) Dot plots displaying serum and nasal NAb titers relative to each other at 6 months after primary mRNA vaccination, at 6 months after booster mRNA vaccination and at 2 to 4 weeks after booster mRNA vaccination in primary AVV-based vaccinated individuals. Lines represent simple linear regression with 95% confidence intervals (CIs) shown in the shaded region. The correlation and significance were tested using a two-tailed Spearman correlation test. **(B)** Violin plots depicting NAb titers in serum (red) and nasal secretions (blue) at baseline and at 2 to 4 weeks or 6 months after primary and booster vaccination in study participants receiving an mRNA-based (red/blue) or AVV-based (gray) vaccine as primary vaccination. All individuals received an mRNA-based booster. Lines show median and quartiles. **(C)** Violin plots depicting serum (red) and nasal (blue) NAb titers at 2 to 4 weeks after primary mRNA vaccination in male and female participants. Significance was determined by Mann-Whitney U test; ns, not significant. Dotted lines in (B) and (C) represents cut-off for neutralization based on pre-coronavirus disease 2019 (COVID-19) samples. LOD, limit of detection.

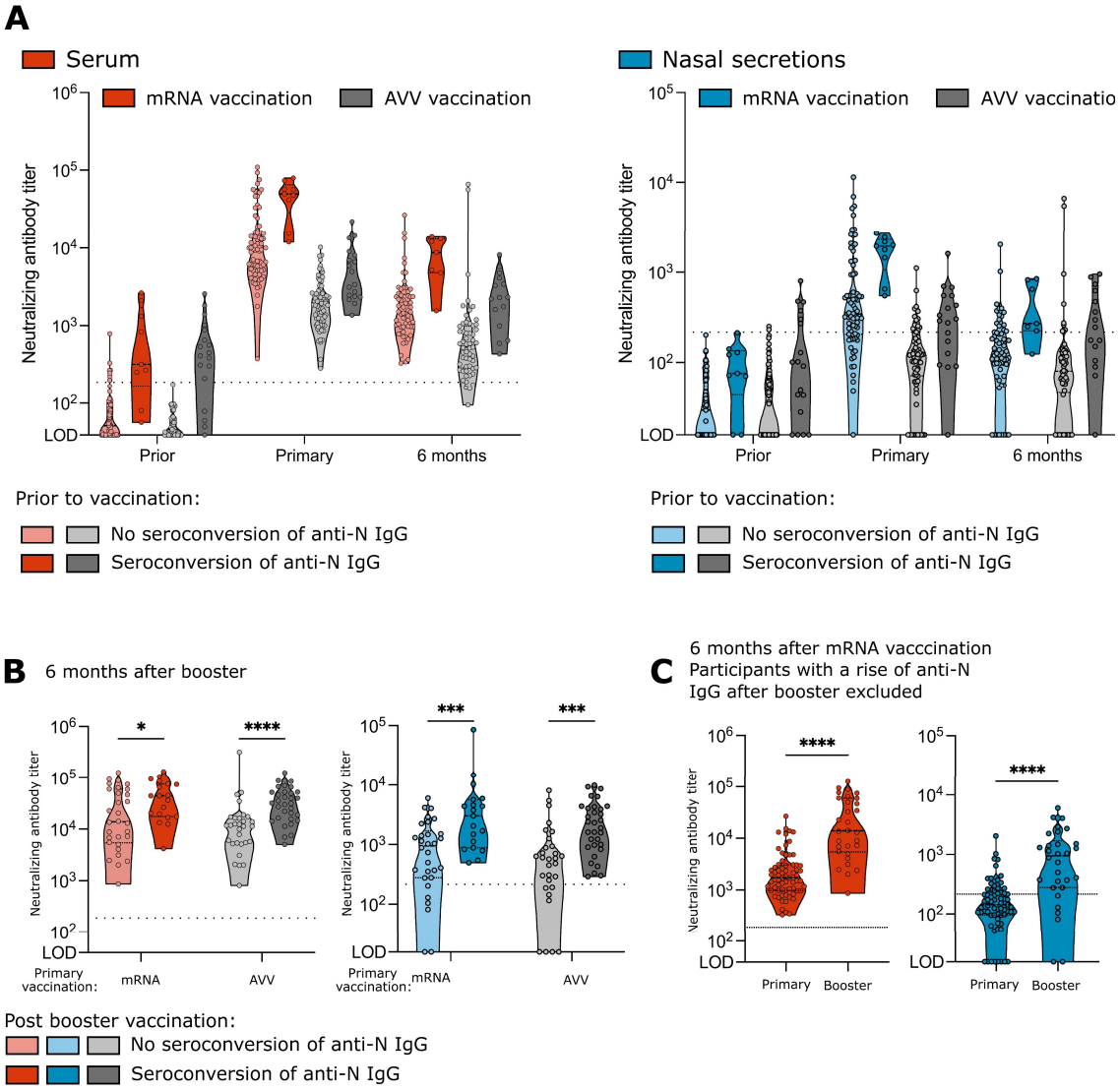

Fig. S2. Effect of COVID-19 on virus NAb titers in the respiratory mucosa.

(A) Violin plots depicting NAb titers in serum (red) and nasal secretions (blue) at baseline and at 2 to 4 weeks or 6 months after primary mRNA- (red/blue) or AVV-based (gray) vaccination. Participants were subdivided based on the presence of serum anti-nucleocapsid (N) IgG prior to vaccination. Participants exhibiting seroconversion of anti-N IgG during the 6-month time course after primary vaccination were excluded from this analysis. **(B)** Virus NAb titers in

serum (red) and nasal secretions (blue) at 6 months after mRNA booster vaccination in participants primary vaccinated with either an mRNA- (blue/red) or AVV-based (gray) vaccine. Participants are grouped in those with and without evidence of natural SARS-CoV-2 infection after booster vaccination (defined as a substantial rise in anti-N IgG serum titer at 6 months post booster compared to 2 to 4 weeks post booster). Participants with raised serum anti-N IgG at 2 to 4 weeks after booster were excluded from the analysis. **(C)** Virus NAb titers in serum (red) and nasal secretions (blue) at 6 months after primary versus booster vaccination in participants vaccinated with mRNA-based vaccines. Participants with a rise in serum anti-N IgG titers after booster vaccination (either at 2 to 4 weeks or 6 months) were excluded from this analysis. All data are represented by violin plots with lines depicting the median and quartiles, and the dotted line representing the cut-off for neutralization based on pre-COVID-19 samples. Significance was determined by Mann-Whitney U test with Holm-Sidak method for multiple testing for (B). *$p < 0.05$, ***$p < 0.001$, and ****$p < 0.0001$.

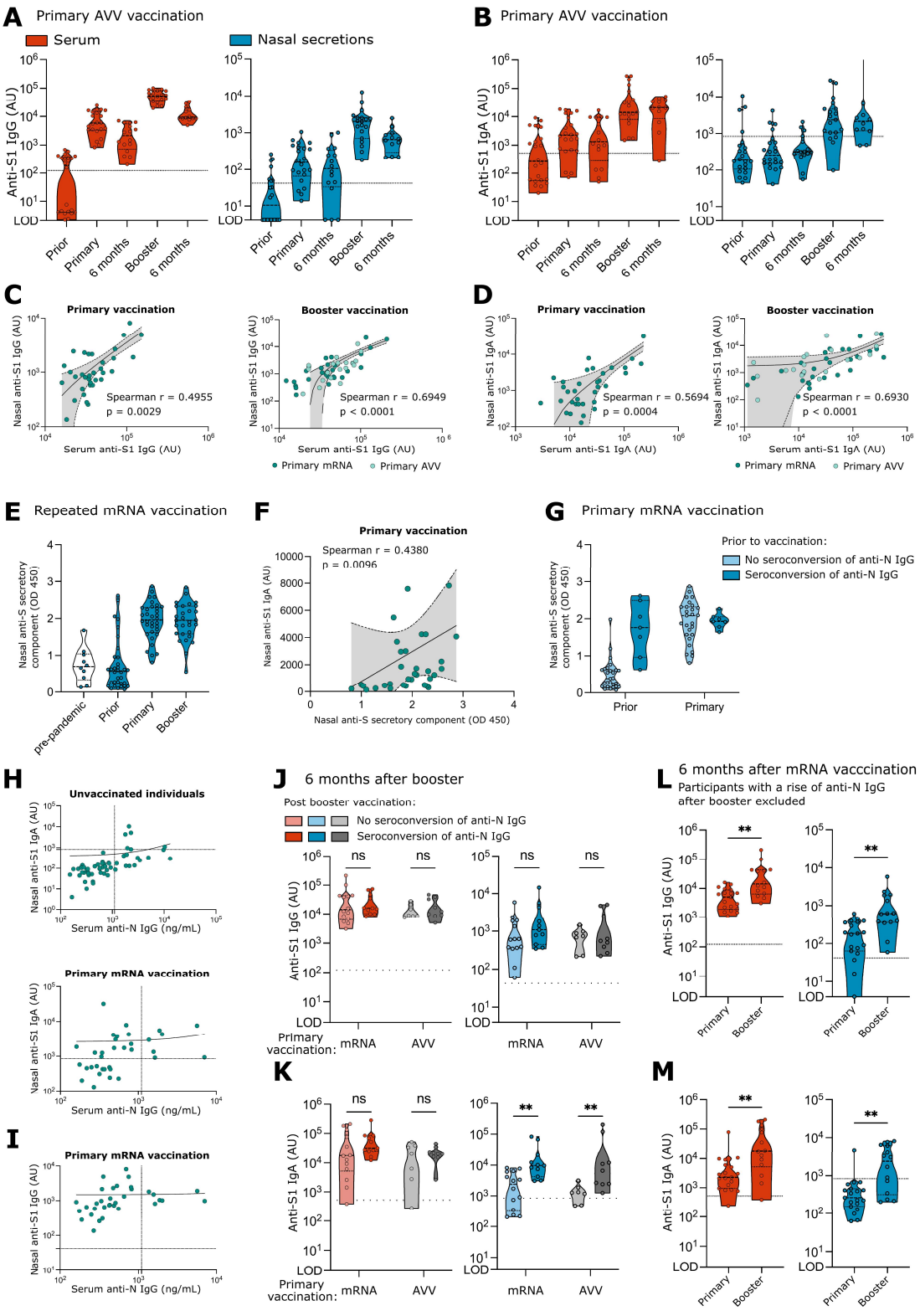

Fig. S3. Kinetics of anti-receptor binding domain (RBD) IgG and IgA in serum and nasal secretions.

(A and B) Violin plots depicting anti-S1 IgG (A) and IgA (B) titers in serum (red) and nasal secretions (blue) at 2 to 4 weeks and 6 months after primary AVV-based and booster mRNA-based vaccination. AU, arbitrary units. **(C and D)** Dot plots displaying serum and nasal anti-S1 IgG (C) and IgA (D) relative to each other at 2 to 4 weeks after primary mRNA-based vaccination and 2 to 4 weeks after booster mRNA-based vaccination. For plots after booster vaccination, participants were subdivided according to mRNA- (dark dots) or AVV-based (light dots) primary vaccination. Lines represent simple linear regression with 95% CIs. The correlation and significance were tested using a two-tailed Spearman correlation test. **(E)** Violin plot depicting anti-S secretory component antibodies in pre-pandemic nasal secretions and in nasal secretions of individuals vaccinated by repeated mRNA-based vaccination at 2 to 4 weeks post primary and booster vaccination. **(F)** Dot plot displaying nasal anti-S1 IgA and nasal anti-S secretory component antibody titers relative to each other at 2 to 4 weeks after primary mRNA vaccination. Lines represent simple linear regression with 95% CIs. The correlation and significance were tested using a two-tailed Spearman correlation test. OD, optical density. **(G)** Violin plot depicting anti-S secretory component antibodies in nasal secretions prior and 2 to 4 weeks post primary mRNA-based vaccination. Participants are subdivided based on the presence of serum anti-N IgG prior to vaccination. **(H)** Dot plots displaying serum anti-N IgG titers relative to nasal anti-S1 IgA titers in unvaccinated individuals (both mRNA and AVV cohort pooled) and at 2 to 4 weeks post the second dose of primary mRNA-based vaccination. Solid line represents simple linear regression. Dotted lines represent cut-off based on pre-COVID-19 samples. **(I)** Dot plot displaying serum anti-N IgG titers to nasal anti-S1 IgG titers in mRNA vaccinated individuals at 2 to 4 weeks after the second vaccination dose. Solid line represents simple linear regression. Dotted lines represent cut-off based on pre-COVID-19 samples. **(J and K)** Violin plots depicting anti-S1 IgG (J) and IgA (K)

concentrations in serum (red) and nasal secretions (blue) at 6 months after mRNA-based booster vaccination in participants with primary mRNA- or AVV-based vaccination. Participants are grouped in those with and without evidence of natural SARS-CoV-2 infection after booster vaccination (defined as a rise in anti-N IgG serum titer at 6 months post booster compared to 2 to 4 weeks post booster). Participants with raised serum anti-N IgG at 2 to 4 weeks after booster were excluded from the analysis. **(L and M)** Violin plots depicting anti-S1 IgG (L) and IgA (M) in serum (red) and nasal secretions (blue) at 6 months post primary versus booster vaccination in individuals vaccinated with mRNA-based vaccines. Participants with a rise in serum anti-N IgG titers after booster vaccination (either at 2 to 4 weeks or 6 months) were excluded from this analysis. All data are represented by violin plots with lines depicting the median and quartiles, and the dotted line representing the cut-off for neutralization based on pre-COVID-19 samples. For violin plots, lines depict the median and quartiles, and dotted line represents the cut-off for neutralization based on pre-COVID-19 samples. Significance was determined by Mann-Whitney U test with Holm-Sidak method for multiple testing for (E) and (F). **$p < 0.01$; ns, not significant. S1, S1 domain of the spike protein.

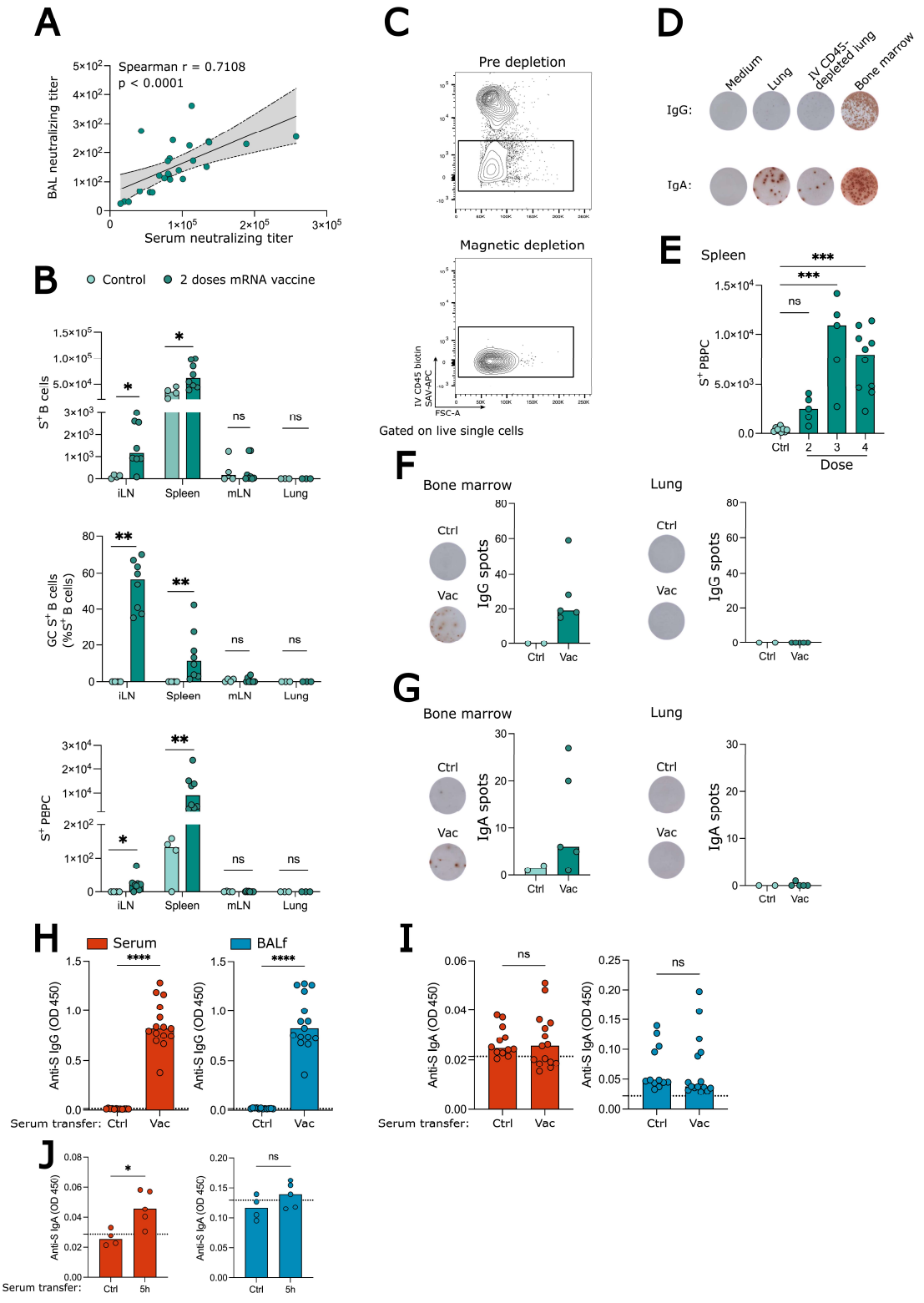

Fig. S4. Repeated mRNA vaccination induces serum virus neutralizing antibodies that can traffic to the respiratory mucosa.

Mice were repeatedly immunized intramuscularly (right leg) with the BNT162b2 vaccine. **(A)** Dot plot displaying serum and bronchoalveolar lavage (BAL) NAb titers relative to each other in mice immunized 1, 2, 3, or 4 times with mRNA vaccination and euthanized at 21 days after the last immunization. Lines represent simple linear regression with 95% CIs. The correlation and significance were tested using a two-tailed Spearman correlation test. **(B)** Number of S-specific B cells, fraction of germinal center (GC) B cells among the S-specific B cells, and S-specific plasmablasts/plasma cells (PBPC) in the draining inguinal lymph node (iLN), spleen, non-draining mediastinal lymph node (mLN), and lung of mice twice vaccinated (n=8) and controls (n=4). Mice were euthanized 7 days after the last immunization. Statistical significance was tested by Mann-Whitney U test. Data are representative of 2 independent experiments. **(C)** Representative flow cytometric validation of magnetically intravenous (IV) $CD45^+$ depleted lung single cell suspensions. Mice were IV labeled by CD45-biotin antibody and lung single cell suspensions were magnetically depleted with streptavidin (SAV)-beads. FSC-A, forward scatter area; APC, allophycocyanin. **(D)** Validation of enzyme-linked immunosorbent spot assay (ELISPOT). Representative images of ELISPOTs to detect IgG and IgA producing plasma cells in lungs that were IV CD45 depleted or not and in bone marrow. ELISPOT plates were coated with anti-light chain κλ. **(E)** S-specific PBPC ($CD138^+CD19^{-/intermediate}$) in spleen of control (Ctrl) mice (n=9) and mice vaccinated 2 (n=5), 3 (n=5) or 4 (n=10) times. Significance was tested by Kruskal-Wallis test with Dunn's correction for multiple testing. **(F and G)** Representative images (left) and quantification (right) of ELISPOTs to detect S-specific IgG (F) and IgA (G) secreting cells in bone marrow and lungs from naïve (n=2) and twice vaccinated (Vac) (n=5) mice. Mice were euthanized 21 days after the last immunization. Lung single cell suspensions were magnetically depleted of IV-labeled cells (CD45 biotin). Data are pooled from 2 independent experiments. **(H and I)** S-specific IgG (H) and S-specific IgA (I)

in serum (red) and BAL fluid (BALf, blue) of adoptively transferred mice with serum from control and vaccinated mice. Mice were euthanized 20 hours after serum transfer. Dotted line represents OD value of blanks. Data are pooled from 2 independent experiments. **(J)** S-specific IgA in serum (red) and BALf (blue) of adoptively transferred mice with serum from control and vaccinated mice. Mice were euthanized 5 hours after serum transfer. Dotted line represents OD value of blanks. Statistical significance in (H to J) was tested by Mann-Whitney U tests. *p < 0.05, **p<0.01, ***p < 0.001, ****p < 0.0001; ns, not significant.

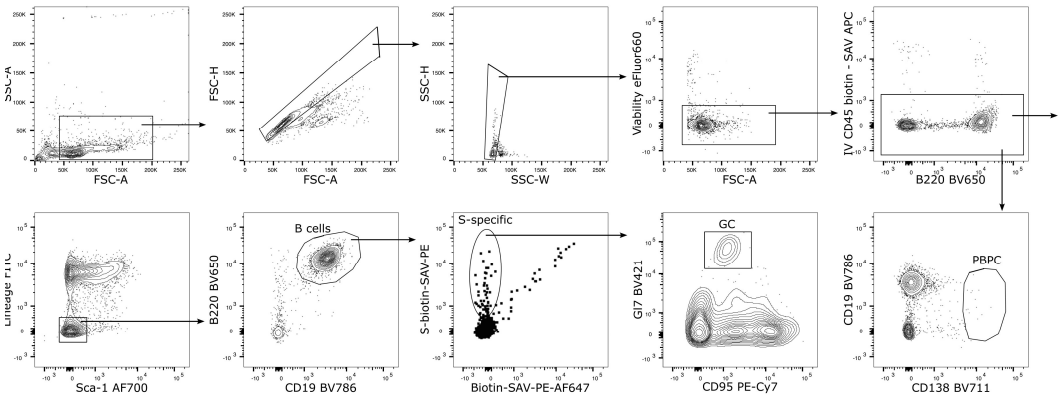

Fig. S5. Representative gating strategy.

SSC-A, side scatter area; FSC-H, forward scatter height; SSC-W, side scatter width; FITC, fluorescein isothiocyanate; AF, Alexa fluor; BV, brilliant violet; PE, phycoerythrin; Cy, cyanine; S, spike protein; GC: germinal center; PBPC: plasmablast / plasma cells.

Table S1. Characteristics of the study population. Data are number of participants n (%), or median (interquartile range, IQR). Participants were asked to report biological sex.

Characteristic	Total 183 (100%)	Primary mRNA vaccination 84 (46%)	Primary AVV vaccination 99 (54%)
Sex			
Male	46 (25%)	23 (27%)	23 (23%)
Female	134 (73%)	61 (73%)	73 (74%)
Prefer not to report	3 (2%)	0 (0%)	3 (3%)
Age	38 (28;48)	41 (30;57)	37 (27;44)
Body mass index (kg/m2)	24	24	24
Current smoking	15 (8%)	8 (10%)	7 (7%)
Comorbidities			
Diabetes mellitus	0 (0%)	0 (0%)	0 (0%)
Cardiovascular disease	3 (2%)	2 (2%)	1 (1%)
Immunodeficiency	2 (1%)	1 (1%)	1 (1%)
Chronic kidney failure	0 (0%)	0 (0%)	0 (0%)
Booster mRNA vaccination			
Total receiving booster	142 (78%)	62 (74%)	80 (81%)
BNT162b2 booster	134 (94%)	59 (95%)	75 (94%)
mRNA-1273 booster	8 (6%)	3 (5%)	5 (6%)
Seroconversion of anti-N IgG			
Prior to primary vaccination	28 (15%)	9 (11%)	19 (19%)
Between primary and booster vaccination	12 (7%)	4 (5%)	8 (8%)
After booster vaccination	50 (45%)	19 (39%)	31 (50%)
Time between vaccination and sampling			
Primary vaccination and first sampling	18 (15;26)	18 (15;22)	22 (15;28)
Primary vaccination and 6 months follow-up	181 (175;189)	182 (175;190)	181 (175;188)
Booster vaccination and first sampling	25 (19;36)	22 (19;31)	27 (20;38)
Booster vaccination and 6 months follow-up	178 (172;190)	176 (172;186)	178 (172;195)

Data Files

Data file S1. Data collected from the human cohort (Fig. 1 and 2)

Data file S2. Data collected from the subgroup human cohort (Fig. 3)

Data file S3. Mouse data (Fig. 4)